Retromer- and WASH-dependent sorting of nutrient transporters requires a multivalent interaction network with ANKRD50

Arunas Kvainickas[1,2], Ana Jimenez Orgaz[1,2], Heike Nägele[1,2], Britta Diedrich[1,2], Kate J. Heesom[3], Jörn Dengjel[4], Peter J. Cullen[3] and Florian Steinberg[1,2,*]

ABSTRACT

Retromer and the associated actin-polymerizing WASH complex are essential for the endocytic recycling of a wide range of integral membrane proteins. A hereditary Parkinson's-disease-causing point mutation (D620N) in the retromer subunit VPS35 perturbs retromer's association with the WASH complex and also with the uncharacterized protein ankyrin-repeat-domain-containing protein 50 (ANKRD50). Here, we firmly establish ANKRD50 as a new and essential component of the SNX27–retromer–WASH super complex. Depletion of ANKRD50 in HeLa or U2OS cells phenocopied the loss of endosome-to-cell-surface recycling of multiple transmembrane proteins seen upon suppression of SNX27, retromer or WASH-complex components. Mass-spectrometry-based quantification of the cell surface proteome of ANKRD50-depleted cells identified amino acid transporters of the SLC1A family, among them SLC1A4, as additional cargo molecules that depend on ANKRD50 and retromer for their endocytic recycling. Mechanistically, we show that ANKRD50 simultaneously engages multiple parts of the SNX27–retromer–WASH complex machinery in a direct and co-operative interaction network that is needed to efficiently recycle the nutrient transporters GLUT1 (also known as SLC2A1) and SLC1A4, and potentially many other surface proteins.

KEY WORDS: SNX27, WASH complex, Endosome, Membrane trafficking, Retromer

INTRODUCTION

The retromer complex is an ancient evolutionary conserved multi-protein assembly that serves as a master organizer of endosomal recycling (Burd and Cullen, 2014; Seaman, 2012). The core of the retromer complex is a constitutive trimer of VPS26, VPS29 and VPS35, which has no intrinsic affinity for membranes, but instead relies on binding to activated RAB7 and various members of the sorting nexin family for its localization to early and maturing later endosomes (Harrison et al., 2014; Seaman et al., 2009, 1998). On these endosomes, retromer orchestrates recycling of internalized transmembrane proteins (cargo) through the generation of actin-decorated and cargo-selective subdomains that prevent entry into the degradative lysosomal pathway (Temkin et al., 2011; Harbour et al., 2010). The actin coat on these recycling domains is generated by the Arp2/3-activating WASH complex, which is recruited onto endosomes through binding of its subunit FAM21 to the retromer subunit VPS35 (Gomez and Billadeau, 2009; Harbour et al., 2012; Jia et al., 2012; Derivery et al., 2009). Although the core retromer trimer itself has an affinity for select cargoes (Fjorback et al., 2012; Seaman, 2007; Tabuchi et al., 2010), it achieves far wider cargo selectivity through recruitment of the PDZ- and FERM-like-domain-bearing cargo adaptor sorting nexin 27 (SNX27) (Temkin et al., 2011; Steinberg et al., 2013). SNX27 is directly bound to the retromer subunit VPS26 and simultaneously binds to a multitude of PDZ- and tyrosine-based sorting motifs in the cytosolic tail of its cargo proteins, thereby driving their recycling back to the cell surface (Steinberg et al., 2013; Gallon et al., 2014; Ghai et al., 2013). Retromer and SNX27 have been shown to recycle a wide range of surface molecules, ranging from signalling receptors like the β2-adrenergic receptor (Lauffer et al., 2010) or the parathyroid hormone receptor (PTHR) (Chan et al., 2016; McGarvey et al., 2016), and nutrient transporters (Steinberg et al., 2013) to neuronal glutamate receptors (Wang et al., 2013; Loo et al., 2014; Hussain et al., 2014). Although loss of retromer as well as of the WASH complex is lethal early in embryogenesis (Wen et al., 2011; Gomez et al., 2012), loss of SNX27 is lethal shortly upon birth of genetically modified mice (Cai et al., 2011), highlighting the physiological relevance of SNX27-, retromer- and/or WASH-driven recycling processes. In this context, recent genome-wide association studies have identified mutations in the retromer subunit VPS35 as the underlying cause for late-onset hereditary Parkinsonism, with the point mutation of aspartate 620 to asparagine (D620N) being the most significant one (Vilarino-Guell et al., 2011; Zimprich et al., 2011). We and others have shown that this point mutation causes a loss of affinity to the WASH complex subunit FAM21, which negatively affects retromer- and WASH-complex-driven recycling and also has effects on autophagy (Zavodszky et al., 2014; McGough et al., 2014c). Our previous quantitative proteomic study suggests that, besides a loss of binding to the WASH complex, the mutant VPS35 also engages to a lesser degree with ankyrin-repeat-domain-containing protein 50 (ANKRD50). ANKRD50 is a large (1429 amino acids) uncharacterized protein that contains 19 ankyrin repeats in its middle and has, besides a C-terminal type-I PDZ-binding motif (threonine, proline, leucine; TPL), no other obvious structural features that could explain its function (Fig. 1A). Its presence in the retromer interactome and a potential role in retromer functionality (McGough et al., 2014a) indicate that the loss of ANKRD50 association with the D620N-mutant VPS35 might well contribute to the development of hereditary Parkinsonism. Here, we characterize ANKRD50 from an in-depth proteomic and cell biology perspective, establishing that ANKRD50 connects with multiple retromer and WASH-complex components in an intricate interaction network that is required for retromer and WASH-complex function.

[1]Center for Biological Systems Analysis (ZBSA), Albert Ludwigs Universitaet Freiburg, Habsburgerstrasse 49, Freiburg 79104, Germany. [2]Faculty of Biology, Schaenzlestrasse 1, D-79104, Freiburg, Germany. [3]School of Biochemistry, Bristol University, University Walk, Bristol BS81TD, UK. [4]Department of Biology, Fribourg University, Chemin du Musee 10, Fribourg CH-1700, Switzerland.

*Author for correspondence (florian.steinberg@zbsa.de)

F.S., 0000-0003-1849-0506

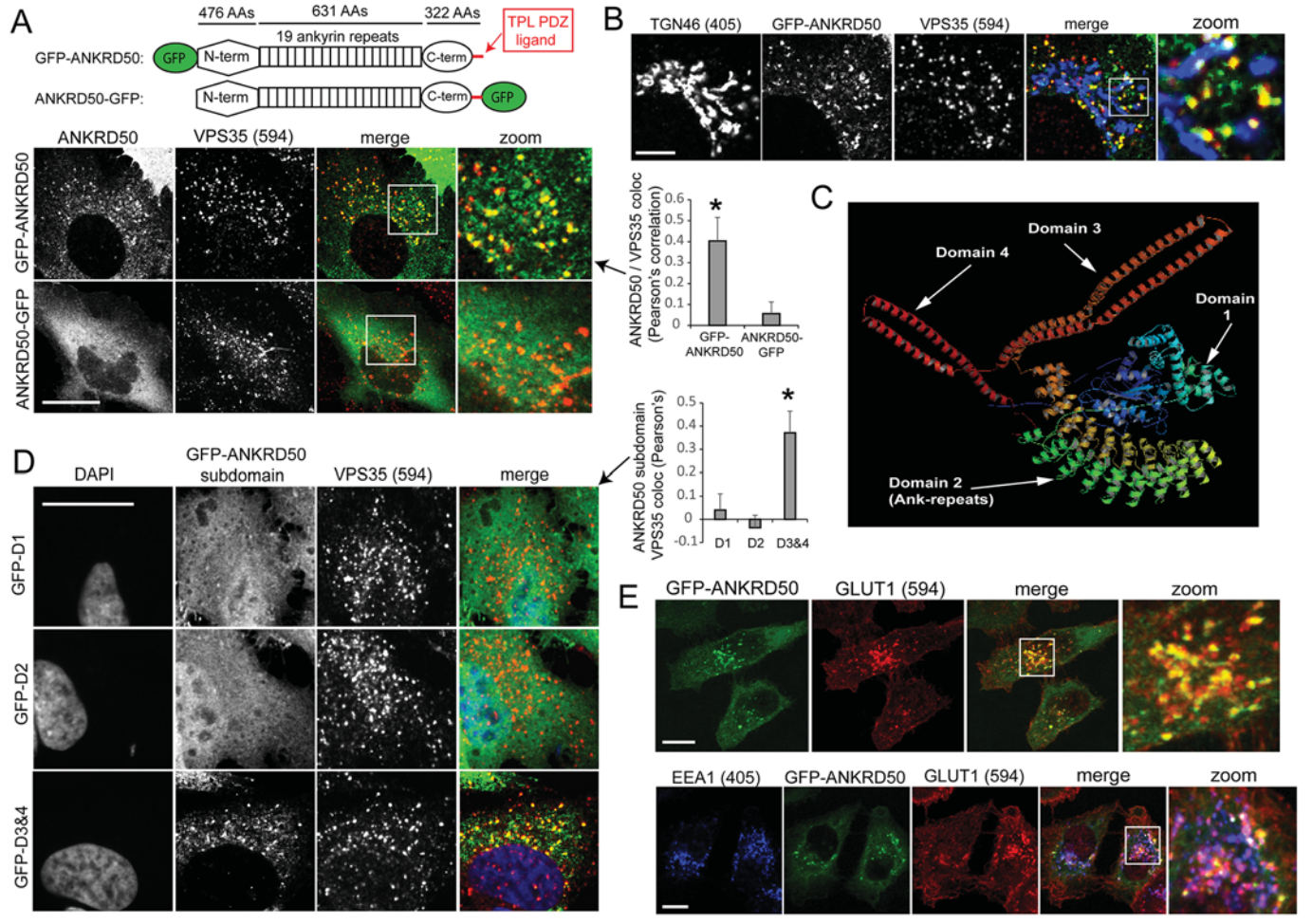

Fig. 1. ANKRD50 localizes to retromer and GLUT1-decorated endosomes through its C-terminus. (A) N- and C-terminally GFP-tagged ANKRD50 constructs were lentivirally expressed using in RPE1 cells and co-stained for endogenous VPS35 (594, red). Colocalization (coloc) was quantified over 20 cells from two independent experiments. (B) Co-staining of TGN46 with endogenous VPS35 and exogenous GFP–ANKRD50 in RPE1 cells. (C) The RaptorX modelling engine was used to generate a model of full-length ANKRD50. (D) GFP-tagged ANKRD50 subdomains (D1=M1–I476, D2=W477–S1112, D3&4=V1113–L1429) were transiently transfected into HeLa cells, which were co-stained for endogenous VPS35. Colocalization between the GFP-tagged domains and VPS35 was quantified over 20 cells from two independent experiments. (E) Lentiviruses were used to express GFP–ANKRD50, which colocalized with internalized endogenous GLUT1 on EEA1-positive endosomal vesicles in HeLa cells. Means are shown. All error bars are s.d. Scale bars: 10 µm. *P<0.05 according to Teacher's t-testing indicating a significant increase in colocalization to D1 and D2. 405, Alexa-Fluor-405, blue.

RESULTS

ANKRD50 is needed to recycle SNX27-, retromer- and WASH-complex-dependent cargo

To analyze ANKRD50 localization, full-length ANKRD50 was expressed using lentiviruses in human retinal pigment epithelium cells (RPE1) as N- and C-terminal GFP-fusion constructs (Fig. 1A). Although a substantial fraction of GFP–ANKRD50 was localized to the cytosol, it could clearly be detected on endosomal vesicles that were decorated with the retromer subunit VPS35 (Fig. 1A). ANKRD50–GFP, in contrast, was cytosolic and did not localize specifically to VPS35-positive endosomes, suggesting that blocking the C-terminal PDZ-binding motif by GFP interfered with its localization. Because of this, N-terminally tagged ANKRD50 was used throughout the study. Co-staining of TGN46 (also known as TGOLN2), a marker for the trans-Golgi network (TGN) showed that GFP–ANKRD50 localized to VPS35-decorated vesicles in a perinuclear area near to the TGN (Fig. 1B). To gain preliminary structural information on ANKRD50, the open reading frame was submitted to various modelling engines. The Raptor-X engine (Kallberg et al., 2012) suggested a highly folded globular N-terminal domain of 476 amino acids [domain 1 (D1)], followed by 19 ankyrin repeats predicted to form a large U-formed domain of 631 amino acids (D2) terminating into two extended helical domains of 179 and 136 amino acids, respectively (called D3&4 here; Fig. 1C). Because of their small size and putative structural similarity, D3&4 were initially treated as one C-terminal domain. The isolated domains were transiently expressed as N-terminal GFP-fusion proteins and analyzed for their localization (Fig. 1D). Domains 1 and 2 displayed cytosolic localization, whereas D3&4 localized to VPS35-decorated vesicles, indicating that ANKRD50 localized to retromer-decorated endosomes through its C-terminal domains. Because SNX27, retromer and the WASH complex promote early endosomal recycling of the glucose transporter GLUT1 (also known as SLC2A1; Steinberg et al., 2013; Piotrowski et al., 2013), we also stained GFP–ANKRD50-expressing cells for endogenous GLUT1. In a subset of cells, ANKRD50 was found to colocalize with early endosomal antigen 1 (EEA1) and with GLUT1-positive vesicles in a perinuclear region (Fig. 1E). Overall,

the localization data suggested that ANKRD50 can localize to retromer- and recycling-cargo-enriched endosomes in a perinuclear area near the TGN through its C-terminal domains.

Depletion of ANKRD50, SNX27, retromer (VPS35) or the WASH-complex subunit FAM21 in human U2OS cells led to pronounced lysosomal mis-sorting of GLUT1, which is normally localized to the cell surface (Fig. 2A). All knockdowns led to almost complete redistribution of endogenous GLUT1 from the plasma membrane to LAMP1-positive lysosomes. The same effect was observed upon suppression of ANKRD50, SNX27 or VPS35 in HeLa cells (Fig. 2B; all channels in Fig. S1A). Five distinct small interfering (si)RNAs against ANKRD50 resulted in similar GLUT1 phenotypes (Fig. S1A), arguing against off-targets effects. In support of lysosomal mis-sorting, knockdown of ANKRD50, SNX27 and VPS35 in U2OS cells resulted in decreased stability of GLUT1 in biotinylation-based degradation assays over 24 and 48 h (Fig. 2C). Importantly, lysosomal mis-sorting of GLUT1 upon ANKRD50 depletion could be rescued by lentiviral re-expression of siRNA-resistant GFP–ANKRD50 (Fig. 2D; all channels in Fig. S1B).

We next examined whether ANKRD50 has retromer-specific or rather more general roles within the endo-lysosomal network. Depletion of ANKRD50 did not result in gross alterations of the size, number and localization of SNX1- and VPS35-decorated sorting endosomes (Fig. S1C), and did not lead to obvious changes in the size and number of SNX1-positive tubules that emanated from these endosomes. Knockdown of ANKRD50 did not lead to gross morphological changes of lysosomes (Fig. S2A) or of the endocytic recycling compartment that had been labelled with fluorescent transferrin (Fig. S2B). Uptake of transferrin over 30 min was slightly increased upon knockdown of ANKRD50 in U2OS cells, but subsequent recycling kinetics over 15, 30 and 45 min were unchanged compared to in control cells (Fig. 3A). EGF-induced degradation of the endogenous EGF receptor (EGFR) in HeLa cells was also unperturbed in ANKRD50-depleted cells, indicating that lysosomes remained functional (Fig. 3B). Autophagy induction as well as autophagic flux, as shown by the formation and accumulation of lipidated GFP–LC3b (LC3b is encoded by *MAP1LC3B*) in nutrient-starved U2OS cells upon blocking of lysosomal degradation by bafilomycin A was unperturbed upon loss

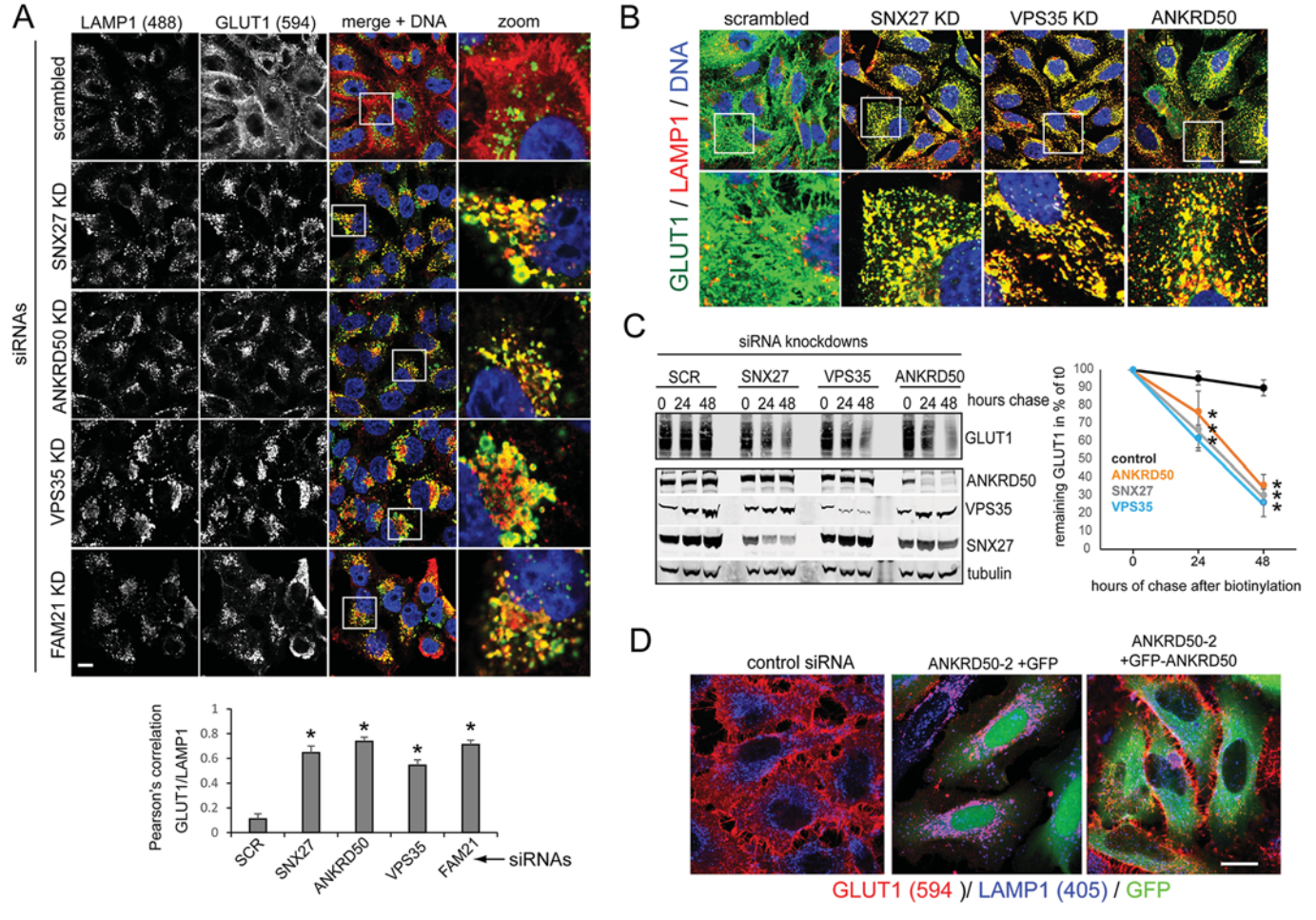

Fig. 2. Depletion of ANKRD50 phenocopies loss of SNX27–retromer–WASH function. (A) U2OS cells that had been transfected with the indicated siRNAs (KD) were stained for endogenous GLUT1 (Alexa-Fluor-594, 594) and the lysosomal marker LAMP1 (Alexa-Fluor-488, 488). Colocalization between GLUT1 and LAMP1 was quantified over 20 images per condition containing hundreds of cells acquired from two independent experiments. SCR, scrambled. (B) HeLa cells were transfected with the indicated siRNAs and stained for endogenous GLUT1 (Alexa-Fluor-488) and endogenous LAMP1 (Alexa-Fluor-594). (C) U2OS cells were transfected with the indicated siRNAs, and cell surface proteins were biotinylated, followed by incubation over 24 and 48 h. Biotinylated proteins were isolated with streptavidin–Sepharose, and biotinylated endogenous GLUT1 was quantified by western blotting. GLUT1 degradation was quantified across three independent experiments. (D) HeLa cells expressing GFP and siRNA-resistant GFP–ANKRD50 were transfected with the siRNA ANKRD50-2 and stained for endogenous GLUT1 and LAMP1 to test whether GFP–ANKRD50 rescued GLUT1 lysosomal mis-sorting. Means are shown. All error bars are s.d. Scale bars: 10 µm. *P<0.05 according to Teacher's t-testing compared to the scrambled control. 405, Alexa-Fluor-405, blue.

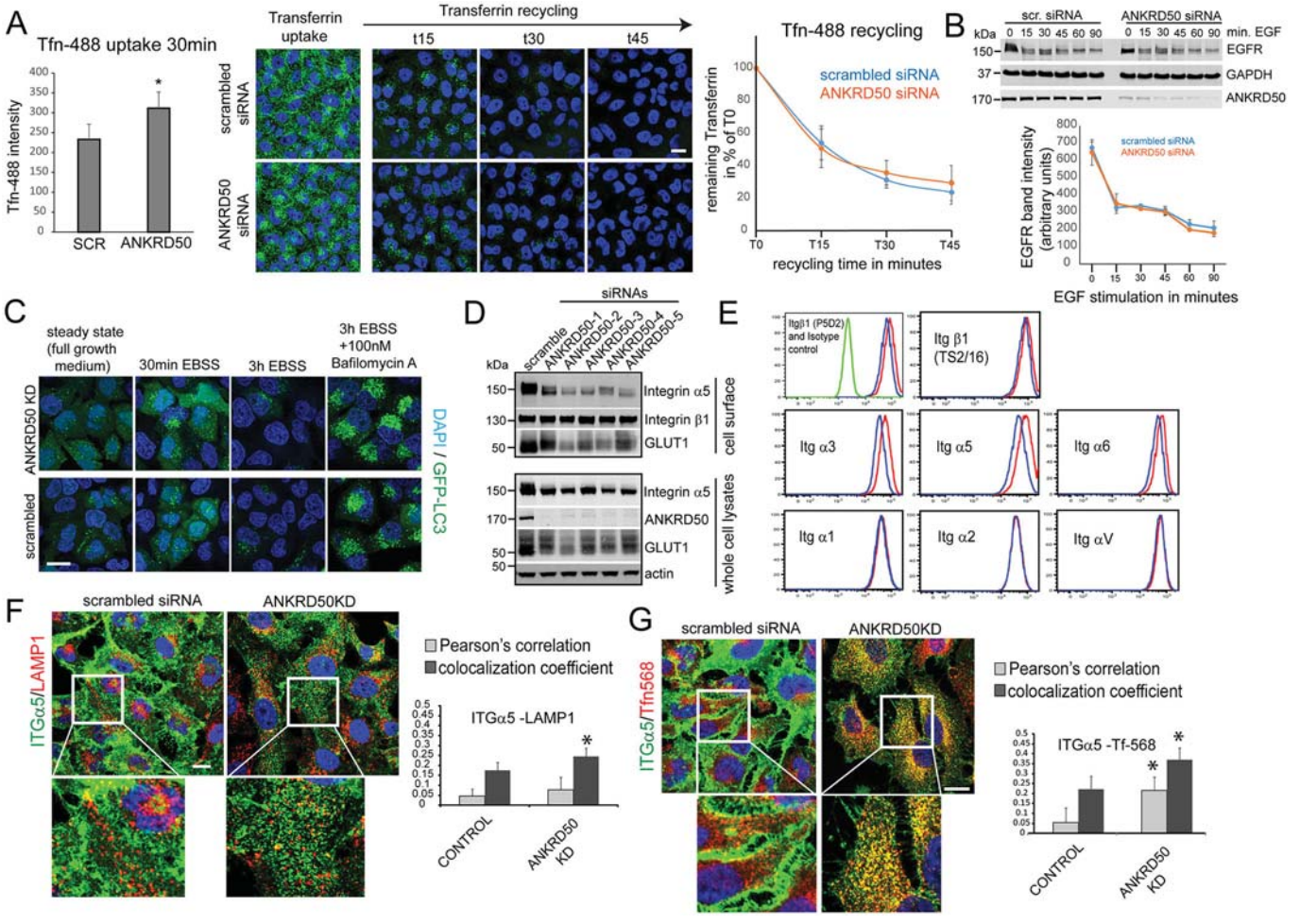

Fig. 3. Effects of ANKRD50 depletion on endosomal tubulation, transferrin recycling, EGFR degradation and integrin recycling. (A) ANKRD50 depletion causes a moderate increase in transferrin (Tfn-488, green) uptake over 30 min but does not affect recycling rates over the indicated time points in U2OS cells. Uptake and recycling rates were quantified over three independent experiments. siRNAs are given on the *x*-axis. SCR, scrambled. (B) Loss of ANKRD50 from HeLa cells does not perturb EGF-induced EGFR degradation. Quantification from three independent experiments is shown. (C) U2OS cells that had been transduced with GFP–LC3b (GFP-LC3) and transfected with control siRNA (scrambled) and siRNA against ANKRD50 (ANKRD50 KD) were starved in EBSS for the indicated time points without and with the lysosomal inhibitor bafilomycin A1 to detect changes in autophagy induction and autophagic flux. (D) HeLa cells that had been transfected with five siRNA oligonucleotides against ANKRD50 (ANKRD50-1 to -5) were assayed for integrin α5β1 surface and total abundance by surface biotinylation and western blotting of surface fractions and total cell lysates. (E) HeLa cells that had been transfected with ANKRD50 siRNA were surface stained with the indicated monoclonal integrin-specific antibodies, and surface abundance was analyzed by flow cytometry. Histogram from control cells in red, ANKRD50 depletion in blue, isotype control in green. Itg, integrin. TS2/16, monoclonal antibody against active β1-integrin; P5D2, monoclonal antibody against inactive β1-integrin. (F) HeLa cells that had been transfected with the indicated siRNA were stained for endogenous integrin α5 (Alexa-Fluor-488) and LAMP1 (Alexa-Fluor-594), and colocalization was quantified over three independent experiments. (G) HeLa cells that had been transfected with the indicated siRNA were incubated with Alexa-Fluor-568-labelled transferrin for 30 min, and fixed and stained for endogenous integrin α5 (Alexa-Fluor-488). Colocalization was quantified over three independent experiments. Means are shown. All error bars are s.d. Scale bars: 10 µm. **P*<0.05 according to Teacher's *t*-testing compared to control.

of ANKRD50 (Fig. 3C). Overall, the data indicate that ANKRD50 is not essential in maintaining general endo-lysosomal function or morphology but that it instead has a specific role in SNX27-retromer, or WASH-complex function. In order to analyze whether ANKRD50 has an effect not only on SNX27-retromer-dependent cargo but also on cargo that relies on the WASH complex for its sorting, we analyzed the trafficking of integrin α5β1. This integrin heterodimer is retrieved from the lysosomal pathway through SNX17 (Bottcher et al., 2012; Steinberg et al., 2012) and requires the WASH complex for its downstream transport away from SNX17-decorated sorting endosomes. Integrin α5β1 has been shown to accumulate in an endosomal compartment upon depletion of WASH1 but is unaffected by loss of SNX27 or retromer (Zech et al., 2011; Duleh and Welch, 2012; Steinberg et al., 2012). Suppression of ANKRD50 in HeLa cells resulted in a loss of integrin α5 and other β1-integrins from the cell surface in western blotting and flow-cytometry-based assays (Fig. 3D and E). We detected only a small increase in lysosomal localization of integrin α5 in ANKRD50-depleted cells but observed pronounced accumulation into transferrin-positive endosomes (Fig. 3F and G; all channels in Fig. S2C and D), similar to the effects of WASH1 suppression that have been reported previously (Zech et al., 2011).

To gain a more general and unbiased insight into the cargo specificity of ANKRD50, we employed stable isotope labelling with amino acids in cell culture (SILAC) proteomics to globally identify the surface molecules that depend on ANKRD50 for their surface localization. Following SILAC labelling in light-isotope (R0K0) and heavy-isotope (R10K8) medium, ANKRD50 was

efficiently depleted from U2OS cells that had been grown in light-isotope medium (Fig. 4A). Biotinylated surface proteins were then quantified using liquid-chromatography-coupled tandem mass spectrometry (LC-MS/MS; complete workflow shown in Fig. S3A). In confirmation of our initial analysis of ANKRD50-depleted cells, GLUT1 and several integrins were lost from the cell surface at least 1.4-fold compared to controls. In addition, several nutrient transporters of the SLC1A family, as well as some signalling receptors, were lost from the ANKRD50-depleted cells (Table S1 contains the original proteomic output), many of which

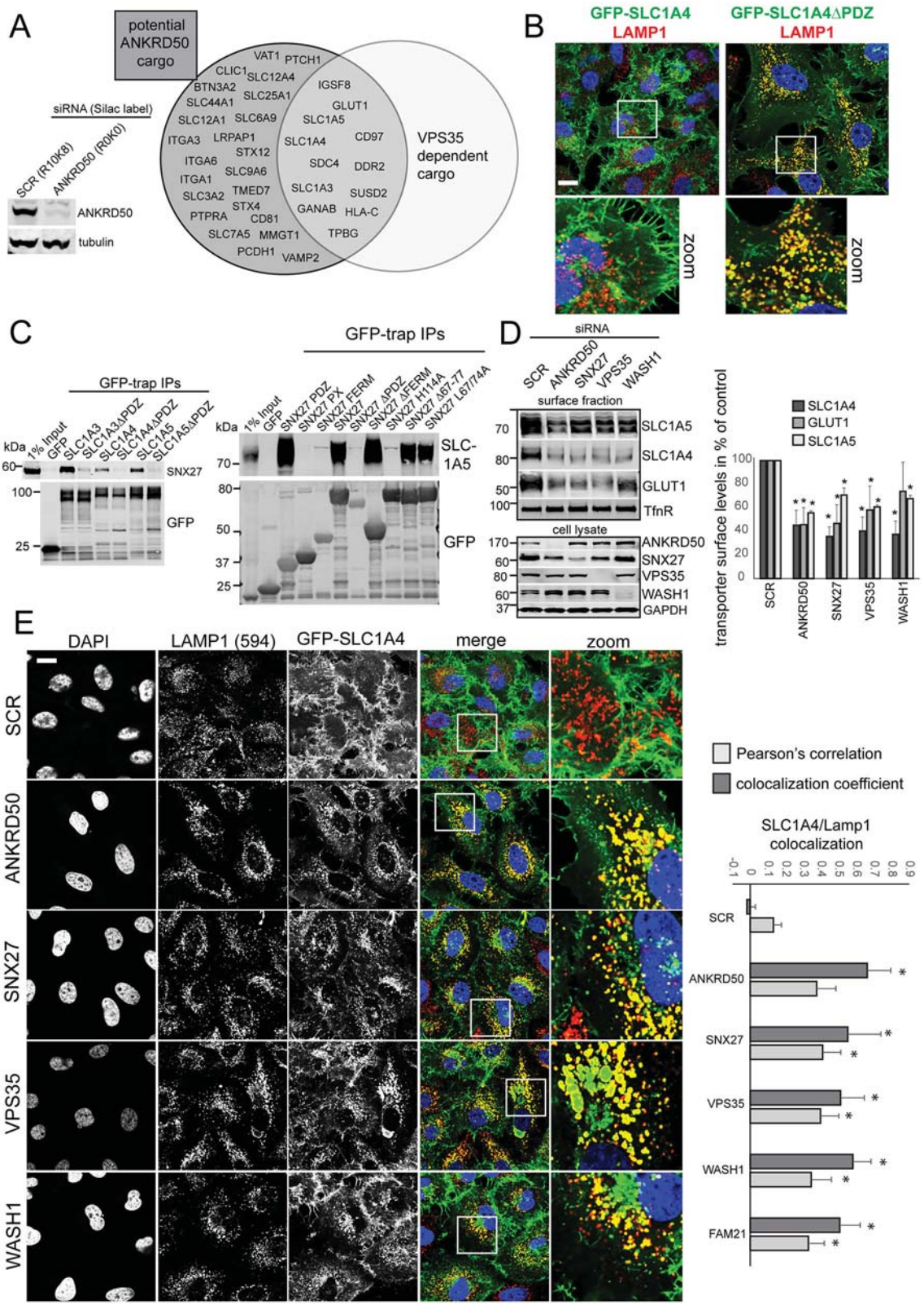

Fig. 4. See next column for legend.

Fig. 4. Proteomic cell surface quantification of ANKRD50-depleted cells identifies amino acid channels of the SLC1A family as ANKRD50-dependent cargoes. (A) SILAC-labelled U2OS cells were depleted of ANKRD50 with siRNA, surface biotinylated and the streptavidin-isolated surface proteins were quantified using LC-MS/MS analysis. The dark grey circle displays all integral membrane proteins that were at least 1.4-fold lower in ANKRD50-depleted cells; the light grey circle shows which of the cargoes have been previously identified as being lost from VPS35-depleted cells. SCR, scrambled siRNA. R10K8, heavy-isotope medium; R0K0, light medium. (B) GFP–SLC1A4 and GFP–SLC1A4ΔPDZ were transiently expressed in HeLa cells, which were then fixed and co-stained for endogenous LAMP1. Blue, DAPI. (C) HEK293 cells were transiently transfected with the indicated GFP-tagged SLC1A-family members, and GFP was precipitated by GFP-trap immunoprecipitation followed by western-blot-based detection of endogenous SNX27 in the precipitates. PX, Phox homology domain. (D) HeLa cells that expressed GFP–SLC1A4 were transfected with the indicated siRNAs, and surface proteins were biotinylated. Streptavidin-isolated endogenous GLUT1, SLC1A5 and GFP–SLC1A4 were then detected by western blotting. The transferrin receptor (TfnR) serves as a loading control for the surface fractions. The quantification was performed over three independent experiments. Band intensity was measured and compared to the band intensity from the SCR control group, and expressed as the percentage of the SCR control group. (E) HeLa cells that had been transduced with GFP–SLC1A4 were transfected with the indicated siRNAs (left-hand labels) and stained for endogenous LAMP1 (Alexa-Fluor-594, 594, red). Blue, DAPI. Quantification of colocalization was performed across three independent experiments. Means are shown. All error bars are s.d. Scale bars: 10 µm. *P<0.05 compared to scrambled control according to Teacher's t-testing.

were also lost from the cell surface proteome of retromer (VPS35)-deficient cells that has been published previously (Steinberg et al., 2013). In order to verify whether some of the putative cargo molecules identified by our proteomic screening were indeed ANKRD50 dependent, we focused on the amino acid transporters of the SLC1A family. Three of its members, SLC1A3, SLC1A4 and SLC1A5 appeared to be lost from the surface of ANKRD50-depleted cells and also display type-I PDZ motifs at their C-termini, making them bona fide SNX27- and/or retromer- and, potentially, WASH-complex-dependent cargo. To verify this, SLC1A4, which showed the most pronounced loss from the surface of ANKRD50- (threefold) and VPS35- (twofold) depleted cells in the mass spectrometry screen, was expressed as an N-terminal GFP-fusion protein with the intact PDZ ligand and without the last three amino acids (GFP–SLC1A4ΔPDZ). Although GFP–SLC1A4 displayed cell surface localization, the ΔPDZ construct localized to lysosomes (Fig. 4B), indicating that the PDZ ligand is needed for endocytic recycling of the transporter, which could be SNX27 dependent. Indeed, all three full-length transporters precipitated endogenous SNX27, which was abolished when the PDZ ligand was removed from the C-terminus (Fig. 4C, left). Full-length SNX27 and the isolated PDZ domain also efficiently precipitated endogenous SLC1A5, whereas deletion (ΔPDZ) or mutation (H114A) of the PDZ domain abolished the interaction (Fig. 4C, right). Truncation of the SNX27 FERM-like domain and mutation of the retromer-binding site within the PDZ domain (Δ67–77) did not perturb SLC1A5 binding, indicating that SNX27 binds to the SLC1A5 PDZ-binding motif through its PDZ domain in a retromer-independent manner (Fig. 4C, right). Finally, depletion of ANKRD50, VPS35 as well as of WASH-complex component WASH1 resulted in a loss of SLC1A4 and SLC1A5 from the cell surface, similar to the loss of the SNX27 and retromer cargo GLUT1 (Fig. 4D). This loss was due to lysosomal mis-sorting given that GFP–SLC1A4 relocalized strongly from the plasma membrane to lysosomes in cells that had been depleted of ANKRD50, SNX27, VPS35 or WASH1 (Fig. 4E). Overall, our results indicate that ANKRD50 localizes to retromer-decorated endosomes through its C-terminal domain and is required for SNX27–retromer–WASH-complex-mediated endosome-to-plasma membrane trafficking of PDZ-ligand-bearing transmembrane proteins as well as of several integrins.

ANKRD50 interacts with multiple components of the SNX27–retromer–WASH machinery

To gain mechanistic insight into how ANKRD50 co-operates with retromer, we used lentiviruses to express GFP–ANKRD50 in SILAC-labelled RPE1 and HEK293 cells, and performed quantitative LC-MS/MS-based interactome analysis of GFP-trap-isolated ANKRD50 (Fig. 5A; Table S1). Fig. 5B shows a STRING network analysis of interacting proteins as well as SILAC enrichment factors averaged over the two experiments. Interestingly, ANKRD50 robustly precipitated all components of the SNX27–retromer–WASH complex given that all members of this large multi-protein assembly were heavily enriched with high peptide counts and high-intensity readings. In addition, a network of PDZ-domain-containing proteins (DLG1, LIN7, etc.), the dystroglycan complex (synthrophin, dystrophin, etc.), as well as γ-tubulin and the entire γ-tubulin-ring complex were identified as strong interacting proteins (Fig. 5B). We also performed quantitative interactome analysis of the isolated ANKRD50 domains according to our bioinformatic model of the ANKRD50 domain structure (constructs shown in Fig. 5G). This revealed that the N-terminal domain D1 interacted strongly with the WASH complex because all components of the WASH complex as well as several components of the WASH-complex-associated CCC complex (Phillips-Krawczak et al., 2015) were detected with high enrichment values and high intensity readings (Fig. 5D; Table S1). By contrast, the D3&4 construct, comprising the two C-terminal domains, efficiently precipitated all components of the retromer complex and SNX27, and also engaged the WASH complex with similar enrichment factors but with much lower intensity readings than obtained for D1 (Fig. 5F; Table S1). The 19 ankyrin repeats (D2) precipitated all six members of the γ-tubulin-ring complex as well as CKAP5, a known interactor of this complex (Fig. 5E). Notably, besides MRP4, no transmembrane cargo was detected in the various interactome datasets, suggesting that ANKRD50 is not a cargo-selective adaptor for retromer. Immunoprecipitation of full-length GFP–ANKRD50 (Fig. 5C) and of the isolated domains (Fig. 5G) fully confirmed the specificity and also the respective strengths of the interactions detected by mass spectrometry.

Next, we set out to analyze these interactions in depth, starting with the interaction between ANKRD50 and SNX27. The LC-MS/MS and western blotting data suggested that the C-terminal domains conferred an interaction with SNX27. Co-expression of GFP-tagged ANKRD50-D4 with Cherry–SNX27 in HeLa cells showed that D4 strongly colocalized with SNX27 on early endosomes (Fig. 6A). GFP–SNX27 as well as the isolated PDZ domain efficiently precipitated endogenous ANKRD50, which was lost upon truncation (ΔPDZ) or mutation (H114A) of the PDZ domain (Fig. 6B). The FERM-like domain precipitated ANKRD50 weakly as well, most likely to occur indirectly through the WASH complex as the FERM-like domain strongly binds to the WASH-complex member FAM21 (Steinberg et al., 2013; Lee et al., 2016). Mutant SNX27 that does not bind the retromer subunit VPS26 [SNX27Δ67–77 and the double mutant L67A,L74A (L67/74A)] (Steinberg et al., 2013; Gallon et al., 2014) retained ANKRD50 binding, suggesting that SNX27 binds to ANKRD50 independently of retromer (Fig. 6B). ANKRD50 harbours a PDZ-domain-binding motif (TPL) at its C-terminal tail, and blocking this motif with a

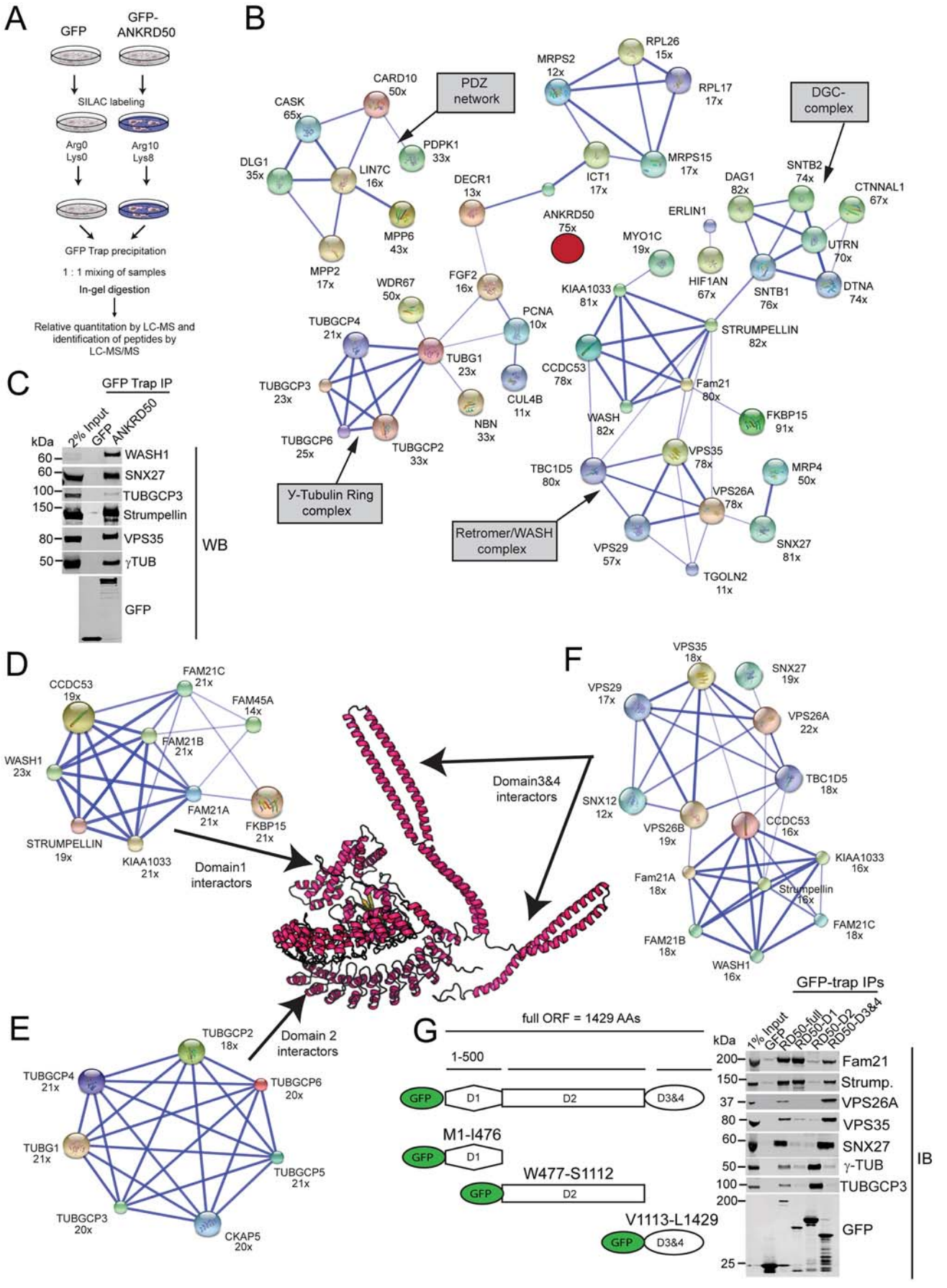

Fig. 5. See next column for legend.

Fig. 5. Mass spectrometry quantification of the ANKRD50 interactome reveals extensive interactions with the retromer and WASH complex. (A) Overview of the SILAC workflow to globally identify binding partners for GFP–ANKRD50 compared to GFP. GFP–ANKRD50 was precipitated from RPE1 and HEK293 cells that had been labelled with heavy-isotope arginine and lysine, followed by LC-MS/MS to identify and quantify binding partners. (B) STRING network analysis of proteins detected in two independent experiments from RPE1 cells and from HEK293 cells. The number below the protein name indicates the fold enrichment over the GFP-only control averaged over the two experiments. (C) HEK293 cells were transiently transfected with GFP–ANKRD50; GFP was isolated by GFP-trap immunoprecipitation and precipitates were analyzed by western blotting of indicated endogenous proteins. (D–F) The isolated GFP-tagged ANKRD50 subdomains were transiently transfected into SILAC-labelled HEK293 cells, and precipitated proteins were quantified by LC-MS/MS. The panels show a STRING network analysis of the identified interacting proteins. The number below the protein name indicates the fold enrichment over the GFP-only control from unlabelled cells detected by the Orbitrap spectrometer. (G) Schematic representation of the overexpressed GFP-tagged subdomains of ANKRD50 (left) and western blot verification of the indicated interacting proteins in subdomain GFP-trap immunoprecipitations from HEK293 cells. IB, immunoblot.

C-terminal GFP tag abolished binding to endogenous SNX27 in HEK293 cells (Fig. 6C). Similarly, deletion of the PDZ ligand from full-length ANKRD50 or from the isolated C-terminal domain also abolished binding to endogenous SNX27 in HEK293 cells (Fig. 6D). Direct recombinant binding assays with Myc-tagged ANKRD50-D4 that had been purified from bacteria and the wild-type PDZ domain, PDZ-binding mutant (H114A) and retromer-binding mutant (Δ67–77) SNX27 PDZ-domain confirmed that ANKRD50 directly bound to the SNX27 PDZ domain through its C-terminal PDZ ligand in a PDZ-binding-pocket-dependent manner (Fig. 6E). In agreement with *in vivo* binding, overexpression of the GFP-tagged C-terminal domain of ANKRD50 (D3&4), but not of D1, D2 or D3&4ΔPDZ constructs, in HeLa cells resulted in lysosomal mis-sorting of endogenous GLUT1 (Fig. 6F) owing to competitive displacement of the GLUT1 PDZ-binding motif from the SNX27 PDZ domain. Notably, GFP–ANKRD50-D3&4, but not the D1 or D2 constructs, localized to endosomal vesicles in these experiments, which was markedly but not completely lost with the D3&4ΔPDZ construct, confirming that the PDZ ligand and a second element in the C-terminus confer endosomal localization of ANKRD50 (Fig. S3B).

Turning towards the ANKRD50–retromer interaction, we first tested where in the C-terminal domain the retromer trimer binds. Splitting of the two C-terminal domains into isolated domains GFP– ANKRD50-D3 and GFP–ANKRD50-D4 and subsequent GFP-trap immunoprecipitations indicated that it is the more-C-terminal D4 that binds retromer (and SNX27) as indicated by the presence of endogenous VPS35 in the precipitates (Fig. 7A). Truncation of the PDZ ligand in the D4 construct abolished binding to SNX27 but left the ability to bind retromer intact (Fig. 7A). Further truncation of the D4 C-terminal amino acids to H1349 revealed that retromer bound in the region between K1295 and H1349 (Fig. 7B). Splitting of this fragment into an N-terminal (residues 1295–1320, D4P1N) and C-terminal part (residues 1321–1349, D4P1C), and subsequent immunoprecipitation of these fragments indicated that the retromer-binding motif was located between amino acids 1295 and 1320 (Fig. S3C). Directed mutagenesis of pairs of amino acids (Fig. 7C) and of individual amino acids to alanine (Fig. 7D) revealed that Y1299, E1300 and M1301, as well as F1304, were essential for retromer binding. Mutation of Y1299 to phenylalanine retained binding (Fig. 7D), ruling out phosphorylation-dependent binding. Conservative mutation of E1300 to glutamine abolished binding, indicating that a negative charge at this position plays a role in binding to retromer. Importantly, in all these experiments, loss of retromer binding also led to a striking loss of SNX27 from the precipitates of these mutants even though the PDZ ligand remained intact, suggesting a high degree of cooperativity between the interactions (Fig. 7C,D). To identify the subunit of the retromer trimer that ANKRD50 binds to, we next precipitated all three overexpressed individual subunits from HEK293 cells. As we have reported previously (Steinberg et al., 2013), only VPS26 efficiently precipitated SNX27, whereas VPS35 was most efficient at precipitating the WASH-complex member strumpellin. All three subunits precipitated endogenous ANKRD50, with most binding to VPS26 and VPS35. Our proteomics screen on the isolated C-terminal part of ANKRD50 (Fig. 4F) suggested that the binding to retromer was direct because no other protein was detected with high enough enrichment and intensity readings to serve as a potential bridging molecule (Table S1, Interactome D3&4). To test this, we expressed the retromer trimer in a HEK293-cell-based secretion system, in which the overexpressed and hemagglutinin (HA)-tagged retromer subunits are co-translationally inserted into the ER lumen and secreted into the tissue culture supernatant without coming into contact with the cytosol in their folded state. GST-tagged ANKRD50-D4 and D4-E1300A were expressed in bacteria, and binding to the full retromer trimer (HA–VPS26, HA–VPS29, HA–VPS35) and to HA–VPS26 and HA–VPS35 in the absence of VPS29 was tested. ANKRD50-D4, but not GST alone, efficiently precipitated the entire trimer, which was greatly reduced with the E1300A mutation. In the absence of VPS29, expression levels of VPS26 and VPS35 were lower, but binding to ANKRD50-D4 was retained, whereas both VPS26 and VPS35 did not bind to GST alone or to the mutant D4-E1300A (Fig. 7F). VPS26 on its own failed to bind to ANKRD50-D4, whereas VPS35 alone bound to ANKRD50-D4, which was largely lost with the E1300A mutation (Fig. S3D). VPS29 alone did not express at detectable levels in this system (data not shown). We conclude that a motif spanning residues Y1299 to F1304 directly binds to VPS35.

Finally, we analyzed the interaction of ANKRD50 with the WASH complex. Confirming binding of the N-terminal domain (D1) to the WASH complex, GFP–ANKRD50-D1 but not D1 that had been split into two equal-sized GFP-fusion constructs efficiently precipitated the WASH-complex member strumpellin, suggesting that the entire domain is needed for binding (Fig. S4A). The WASH complex comprises five proteins, WASH1, CCDC53, KIAA1033, strumpellin and FAM21 (Derivery et al., 2009; Gomez and Billadeau, 2009), and forms a large and constitutive assembly (Fig. 7G). To identify the binding partner for ANKRD50 within this complex, we overexpressed all individual subunits of the complex as GFP-fusion proteins and analyzed precipitates for the presence of endogenous ANKRD50. Only FAM21 precipitated ANKRD50 (Fig. 7G), indicating that this subunit engages ANKRD50. FAM21 comprises a globular N-terminal domain that acts as a scaffold for the other members of the WASH complex (Fig. 7G), whereas its large C-terminal tail (around 1000 residues) is largely unstructured and contains repetitive retromer-binding elements that engage the retromer subunit VPS35 (Jia et al., 2012) and, as recently shown, SNX27 directly (Lee et al., 2016). GFP–FAM21 and GFP–FAM21-tail both precipitated ANKRD50, SNX27 and VPS35 (Fig. S4B), whereas strumpellin was lost from the tail precipitates, confirming that the head region engages the other members of the WASH complex (Jia et al., 2010). Surprisingly, precipitation of the isolated head region as

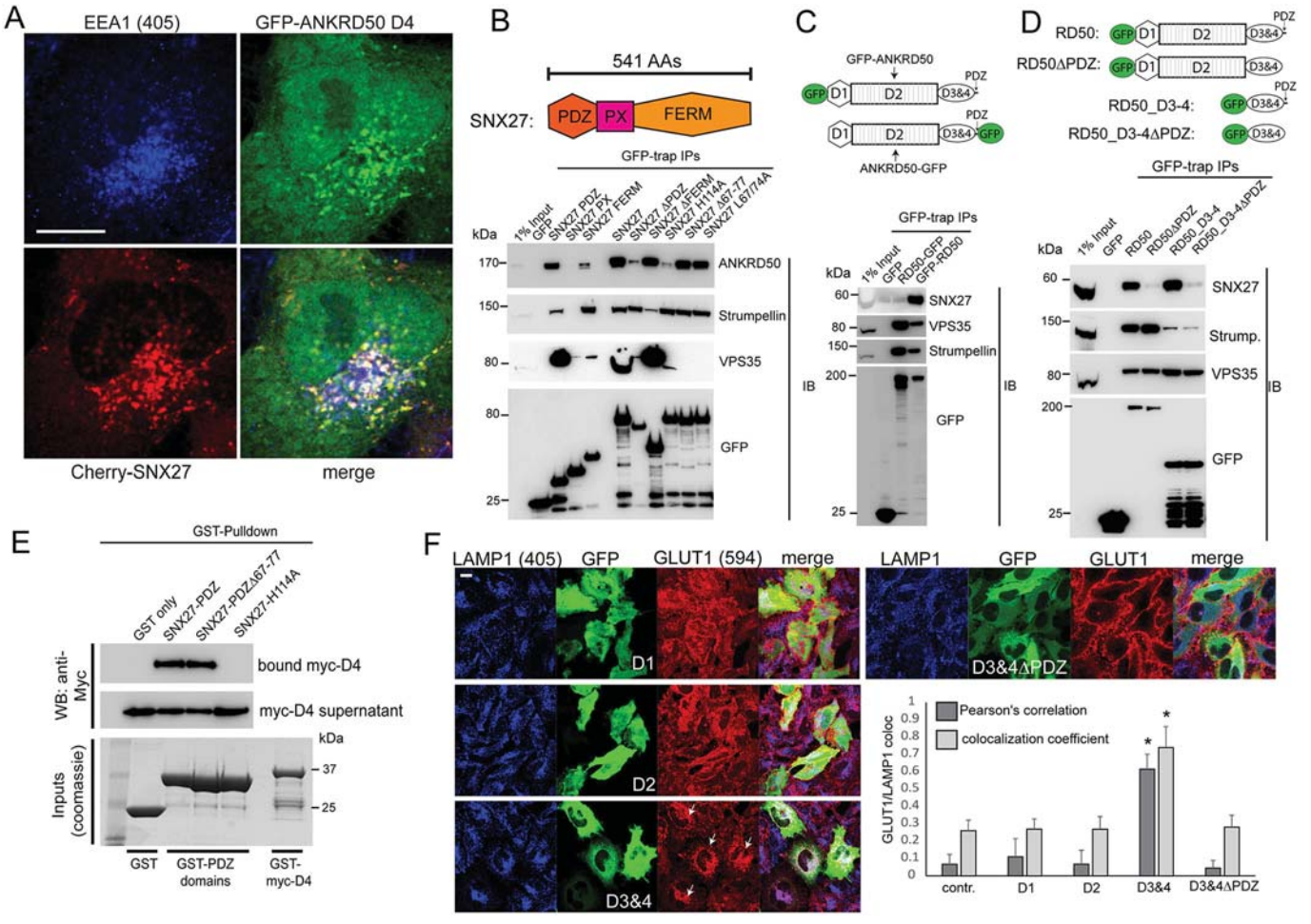

Fig. 6. ANKRD50 directly interacts with SNX27 through a C-terminal PDZ-binding motif. (A) The GFP-tagged C-terminal domain of ANKRD50 (GFP–ANKRD50-D4) colocalized with co-transfected mCherry–SNX27 and endogenous EEA1 (Alexa-Fluor-405, 405) in HeLa cells. (B) HEK293 cells were transiently transfected with the indicated GFP-tagged SNX27 constructs; GFP was isolated through GFP-trap immunoprecipitations, and precipitates were analyzed for the indicated proteins by western blotting. PDZ, PX and FERM=isolated SNX27 subdomains; Δ indicates truncation of the indicated subdomain; H114A=PDZ-binding mutant; Δ67–77 and L67/74A=retromer-binding mutants. AA, amino acid. (C) N-terminally tagged ANKRD50 but not C-terminally GFP-tagged ANKRD50 precipitated endogenous ANKRD50 from transiently transfected HEK293 cells. RD50, ANKRD50. (D) HEK293 cells were transiently transfected with the indicated GFP-tagged constructs, GFP-trap immunoprecipitations were then performed, and detection of the indicated proteins was performed by western blotting (WB, IB). (E) GST- and Myc-tagged ANKRD50-D4 and indicated GST-tagged SNX27 PDZ domains were expressed in bacteria. Myc-D4 was cleaved from the GST tag with Prescission protease and assayed for binding to the GST-tagged PDZ proteins that remained on the beads. H114A=PDZ-binding mutant; Δ67–77=retromer-binding mutant. (F) HeLa cells were transfected with the indicated GFP-tagged ANKRD50 subdomains, and fixed and stained for endogenous GLUT1 (Alexa-Fluor-594) and LAMP1 (Alexa-Fluor-405, 405). Lysosomal localization of GLUT1 was quantified over three independent experiments. Arrows indicate lysosomal GLUT1. Coloc, colocalization. Means are shown. All error bars are s.d. Scale bars: 10 µm. *P<0.05 according to Teacher's t-testing compared to control (contr.).

well as of several FAM21-tail-truncated constructs showed that ANKRD50 was most efficiently precipitated by the head region (Fig. 7H). All the tail constructs, which have been shown previously to contain retromer- and SNX27-binding repeat elements (Jia et al., 2012), also precipitated ANKRD50 alongside retromer and SNX27 (Fig. 7H). This was probably due to indirect interactions in which SNX27 and VPS35 that bound to ANKRD50 was precipitated by the FAM21 tail through these proteins. Confirming our immunoprecipitation data from HEK293 cells, recombinant GST–FAM21-head, but not GST–FAM21-tail, bound to recombinant and purified GFP–ANKRD50-D1 (Fig. 7I), thereby proving a direct interaction of ANKRD50-D1 with the FAM21-head. Overall, our interaction studies revealed an intricate interaction network between ANKRD50 with SNX27–retromer–WASH in which the C-terminal PDZ ligand directly engages SNX27, while the C-terminal D4 directly binds to VPS35 and the N-terminal D1 directly engages the FAM21-head region within the WASH complex (Fig. 7J).

Retromer function requires several distinct interactions with ANKRD50

We next aimed to establish the functional relevance of these individual interactions by analyzing the trafficking of mCherry–SLC1A4 in cells that had been depleted of endogenous ANKRD50 and then transduced with the mutant versions. Fig. 8A depicts the GFP-tagged rescue constructs used for these experiments. GFP-trap precipitation of the rescue constructs confirmed the results of our mapping experiments, as ANKRD50ΔD1 lost the ability to bind to the WASH complex, ANKRD50ΔD2 lost the ability to bind to the γ-tubulin-ring complex, ANKRD50ΔD3&4 and ANKRD50E1300A lost the ability to bind to retromer and SNX27, whereas the ΔPDZ construct was only unable to bind to SNX27 (Fig. 8A). The average knockdown efficiency of endogenous ANKRD50 was around

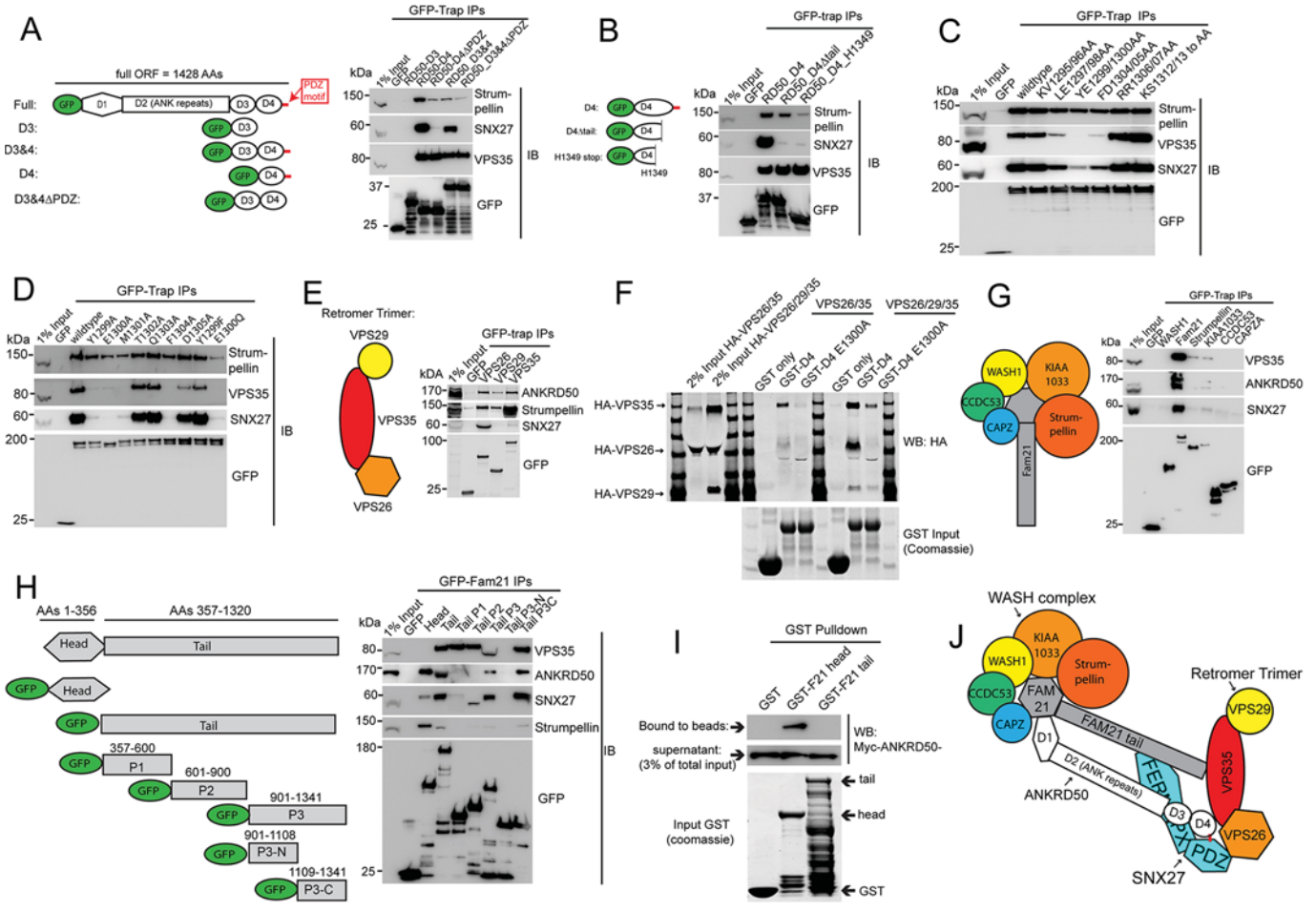

Fig. 7. ANKRD50 directly interacts with the retromer trimer and WASH-complex component FAM21. If not otherwise indicated, panels show western blot (IB, WB) analysis of GFP-trap immunoprecipitations (IPs) of the indicated proteins from transiently transfected HEK293 cells. (A) The isolated D4 [amino acids (AAs) 1293–1429] but not D3 (AAs 1113–1292) of ANKRD50 binds to the retromer trimer (VPS35) independently of SNX27 and the WASH complex (strumpellin). RD50, ANKRD50. (B) Truncation of the D4 C-terminus (D4Δtail=AAs 1293–1412) abolishes SNX27 binding but leaves binding to retromer intact. The N-terminal half of D4 (D4-H1349stop, AAs 1293–1349) is sufficient to precipitate endogenous VPS35. (C) Alanine scanning of amino-acid doublets in full-length ANKRD50 suggests that a stretch of amino acids from L1297 to D1305 is important for binding to retromer. KV1295/96AA, K1295A V1296A; LE1297/98AA, L1297A E1298A; YE1299/1300AA, Y1299A E1300A; FD1304/05AA, F1304A D1305A; RR1306/07AA, R1306A R1307A; KS1312/13 to AA, K1312A S1313A. (D) Alanine scanning of single amino acids (right) revealed that residues Y1299, E1300, M1301 and F1304 are crucial for retromer binding. The conservative Y1299F mutant, but not the E1300Q mutant, retained the ability to bind to retromer. Note that all mutants that lose retromer binding also display decreased WASH-complex and SNX27 binding. (E) Schematic representation of the retromer trimer. All individually overexpressed components of the retromer trimer precipitated endogenous ANKRD50. (F) GST-tagged ANKRD50-D4 but not the retromer-binding mutant GST–D4-E1300A that had been produced in bacteria bound to the pSecTag2-expressed and HA-tagged retromer trimer that had been secreted into the tissue culture supernatant from HEK293 cells (western blot for HA; right-hand lanes). Binding was retained in the absence of VPS29 (western blot for HA, middle lanes). (G) Schematic representation of the WASH complex. Of all individually overexpressed GFP-tagged WASH-complex components, only GFP–FAM21 precipitated endogenous ANKRD50. (H) Precipitation of the indicated FAM21 construct revealed that endogenous ANKRD50 was efficiently precipitated by the head region of FAM21. The indicated tail constructs are likely to precipitate ANKRD50 through SNX27 and VPS35. Note that the large amount of overexpressed GFP–FAM21-tail isolated by GFP-trap pushes down the endogenous ANKRD50 band. (I) The recombinant GST-tagged Fam21 head region but not the tail bound to recombinant Myc-tagged ANKRD50-D1. All shown proteins were produced in bacteria. (J) Schematic model of the interactions between ANKRD50 and the SNX27–retromer–WASH complex as indicated by our mapping efforts. ANK, ankyrin.

85%, and re-expression of siRNA-resistant constructs restored ANKRD50 expression with moderate levels of overexpression (Fig. 8B). These cells were then analyzed for overall SLC1A4 levels by performing confocal microscopy (Fig. 8C, bottom left) and also for lysosomal mis-sorting of SLC1A4 as quantified by measuring colocalization with LAMP1 (Fig. 8C, bottom right). As shown before, depletion of ANKRD50 from the GFP-only-expressing control cells strongly decreased overall SLC1A4 levels owing to lysosomal mis-sorting and degradation of this transporter. Re-expression of ANKRD50 revealed that only full-length GFP–ANKRD50 was able to fully restore SLC1A4 levels and plasma membrane localization (Fig. 8C, image panel). The ΔD1 and ΔD2 constructs were completely devoid of any rescue competency, whereas the retromer- and SNX27-binding mutants ΔD3&4, E1300A and ΔPDZ partially restored SLC1A4 levels and localization. Notably, deletion of the ankyrin repeats resulted in tighter association of GFP–ANKRD50ΔD2 with endosomal vesicles than seen with the other constructs (Fig. S4C). These experiments suggested that D1 and WASH-complex binding, as well as the ankyrin repeats, are crucial for the function of ANKRD50, whereas the C-terminal domains and binding to retromer and SNX27 are important but not fully required for the

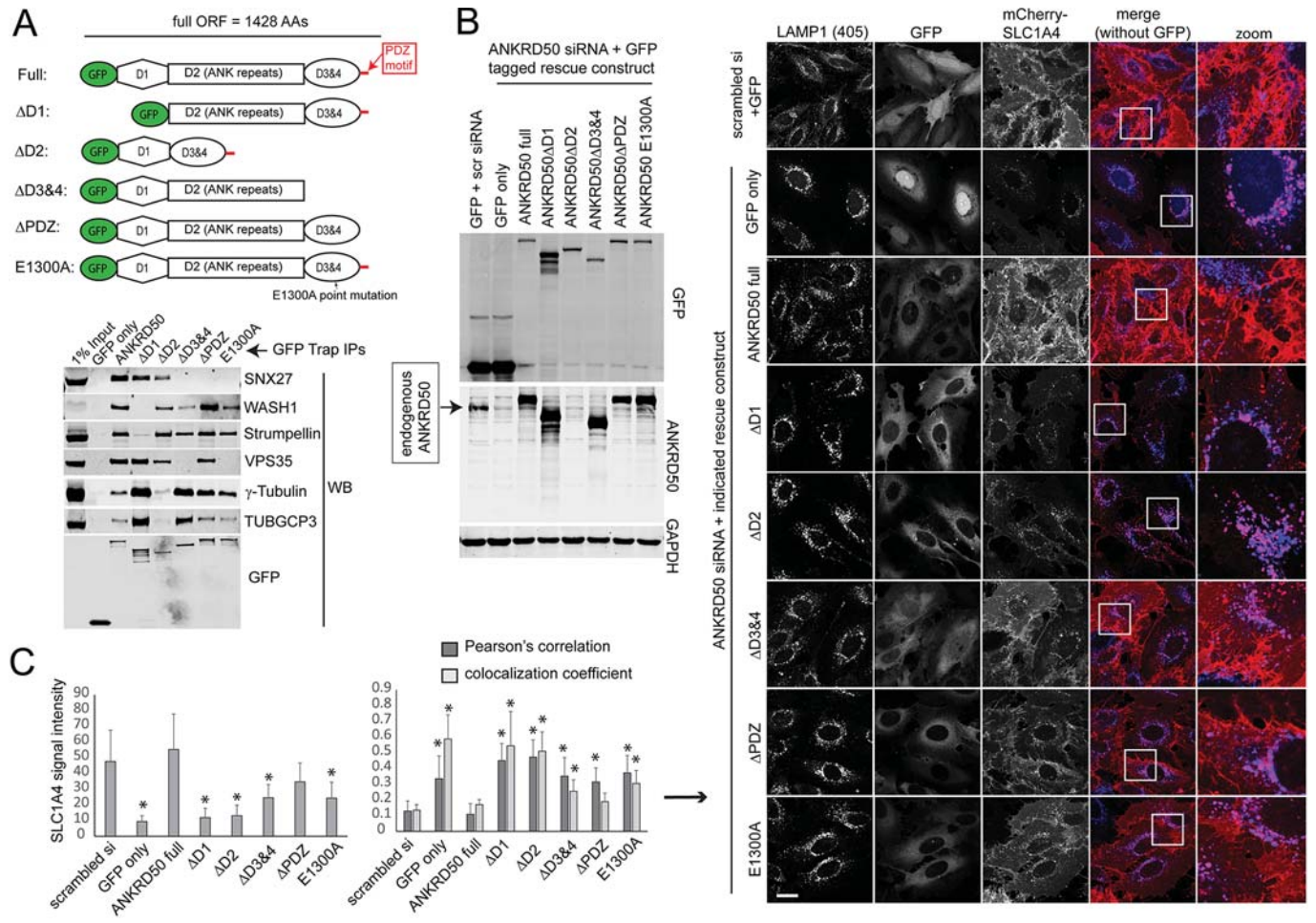

Fig. 8. Knockdown and re-expression experiments reveal that all ANKRD50 interactions are needed for full functionality in endosomal recycling. (A) Schematic representation of all GFP-tagged and siRNA-resistant lentiviral rescue constructs used to rescue SLC1A4 recycling. The western blot panel shows the loss of the respective interacting proteins when the expressed mutant proteins were precipitated using GFP-trap from transduced HeLa cells. (B) HeLa cells were transfected with the ANKRD50-2 siRNA and analyzed by western blotting for the loss of endogenous ANKRD50 and the re-expression of the GFP-tagged lentivirally transduced rescue proteins. Note that the polyclonal antibody against ANKRD50 targets the ankyrin-repeat domain. 405, Alexa-Fluor-405, blue. (C) Staining of mCherry–SLC1A4 (red) and endogenous LAMP1 in HeLa cells that had been depleted of endogenous ANKRD50 and that re-expressed the indicated GFP-tagged mutant versions. The loss of SLC1A4 signal intensity and lysosomal colocalization was quantified in three independent experiments. Means are shown. All error bars are s.d. Scale bars: 10 µm. **P*<0.05 according to Teacher's *t*-testing compared to the scrambled control. ANK, ankyrin; si, siRNA.

role of ANKRD50 in recycling of surface molecules. Overall, our data indicate that multiple interactions of SNX27, retromer and the WASH complex with ANKRD50 are needed for the efficient recycling of SNX27–retromer–WASH-dependent cargo.

DISCUSSION

We establish that the previously uncharacterized protein ANKRD50 can localize to perinuclear endosomal vesicles through multiple direct interactions with components of the SNX27–retromer–WASH complex. There, it is required for SNX27-, retromer- and WASH-complex-mediated recycling of nutrient transporters like the amino acid transporters of the SLC1A family, the glucose transporter GLUT1 and many other surface proteins. Through extensive mapping and mutagenesis of ANKRD50, we further establish that all of the interactions are needed to a different extent to support efficient endosomal recycling through the SNX27–retromer–WASH complex.

ANKRD50 was discovered as a retromer and WASH-interacting protein in our proteomic screen that was designed to detect changes in the interactome of the Parkinson's-disease-causing D620N mutation in the retromer subunit VPS35. The D620N mutation leads to loss of WASH-complex association with the retromer trimer and also causes a decrease of ANKRD50 in VPS35 precipitates, suggesting that ANKRD50 is a WASH-complex-associated protein (McGough et al., 2014b). This assumption needs to be revised as the extensive interaction analysis in this study indicates that the association between ANKRD50 and the SNX27–retromer–WASH complex depends on at least three independent direct interactions: the N-terminal domain directly binds to the head domain of FAM21 in the WASH complex, the C-terminal PDZ-binding motif engages SNX27, whereas the retromer subunit VPS29 interacts with ANKRD50 through a C-terminal motif centred around the amino acid E1300. The interactions appear to strengthen each other in a cooperative way as mutation of the SNX27-binding site consistently decreased WASH-complex binding, whereas mutation of the retromer-binding site resulted in a striking reduction of SNX27 and WASH-complex binding. This cooperativity explains why the D620N mutation in VPS35, which causes a loss of affinity for the WASH-complex component FAM21 (McGough et al., 2014b; Zavodszky et al., 2014), also led to a decrease in ANKRD50

association with the retromer trimer. Given that ANKRD50 is required for retromer and WASH-complex function, its loss from the mutant retromer might well contribute to sorting defects that ultimately cause neuronal death.

Our mutagenesis analysis indicates that either the interaction of the N-terminus with FAM21 or an intrinsic function of the N-terminal domain itself is required for the function of ANKRD50 in the recycling of cargo, as the N-terminally truncated ANKRD50 construct was unable to rescue SLC1A4 recycling. Similarly, the presence of the ankyrin repeats was required for ANKRD50 function given that deletion of the repeats completely abolished recycling of SLC1A4. Mutation of the SNX27- and VPS35-binding site, in contrast, only led to an impairment of ANKRD50 function, suggesting that these interactions either regulate or promote the function of ANKRD50 without being essential. The core functional unit of ANKRD50 thus appears to be the FAM21-associated N-terminal domain along with the 19 ankyrin repeats in the middle region of the protein. It remains to be determined how these two domains of ANKRD50 influence SNX27–retromer- and WASH-complex-mediated sorting on a molecular level. Our detailed proteomic interactome analysis indicates that the N-terminal domain interacts strongly with FKBP15, a largely uncharacterized protein that has been previously shown to also interact with the tail of FAM21 (Harbour et al., 2012). It will be interesting to test the functional relevance of this interaction in the context of retromer and WASH-complex function. It will also be important to investigate the functional relevance of the interaction between the ANKRD50 ankyrin repeats and the γ-tubulin-ring complex, which we detected by using proteomics and verified by western blotting. Although the ankyrin repeats could be needed to recruit important accessory proteins to retromer or the WASH complex, it is also possible that the large and rigid ankyrin-repeat domain, along with the other observed retromer interactions, has a scaffolding function for productive SNX27, retromer and WASH-complex assembly. In this context, the association of the ANKRD50 C-terminal PDZ-binding motif with SNX27 is the most puzzling interaction, as ANKRD50 would block the PDZ-binding pocket of this sorting nexin for SNX27 cargo like GLUT1 or SLC1A4 if it was constitutively bound to it. One possible function could be that ANKRD50 can be recruited by the retromer trimer or the WASH complex, whereupon ANKRD50 displaces SNX27-bound cargo to release the cargo into recycling tubules ready for transport. Our overexpression of the ANKRD50 C-terminus indicates that ANKRD50 can displace GLUT1 from SNX27, making such a scenario conceivable. Overall, our work has established ANKRD50 as a new component of the SNX27–retromer–WASH complex that engages this assembly through an elaborate network of interactions that are required for the recycling of a wide range of integral membrane proteins. With our extensive interactome analysis and the mapping of its interactions, our work should provide a solid base for further research into this interesting new component of the SNX27–retromer–WASH super complex.

MATERIALS AND METHODS

Antibodies

Antibodies used in this study were: rabbit anti-GLUT1 (ab115730), rabbit anti-LAMP1 (ab24170), mouse anti-SNX27 (ab77799), rabbit anti-VPS26A (ab181352) from Abcam; mouse anti-EEA1 (610457), mouse anti-SNX1 (611482) from BD Biosciences; rabbit anti-ANKRD50 (A302-999A, Bethyl); mouse anti-WASH1 (657702, Biolegend); rabbit anti-EGFR (D38B1, Cell Signaling); rat anti-GFP (3H9, Chromotek); rabbit anti-GAPDH (60004-I-Ig); rabbit anti-TUBGCP3 (15179-1-AP); rabbit anti-TUBG1 (15176-1-AP) from Proteintech; mouse anti-β-tubulin (T9026) and anti-VPS35 (SAB2700982) from Sigma-Aldrich. Rabbit anti-strumpellin (sc-87442) from Santa Cruz. For western blotting, all antibodies were used at 1:1000. For immunofluorescence, all antibodies were used at 1:100.

ANKRD50 constructs and mutagenesis

The ANKRD50 open reading frame was cloned from HeLa cell cDNA and transferred into pEGFP-C1, pEGFP-N1 and pLVX puro (all from Clontech). Construct designs were based on information in UniProt database on ANKRD50 (Q9ULJ7) and the RaptorX-generated model of ANKRD50 protein structure. All constructs, including constructed through site-directed mutagenesis, were generated using KAPA HiFi HotStart ReadyMix (KK2602, KAPABIOSYSTEMS), following the manufacturer's guidelines.

Cell culture and transfection

HEK293, U2OS, HeLa and RPE1 (all from American Type Culture Collection) cells were grown in high-glucose Dulbecco's modified Eagle's medium (DMEM; Sigma-Aldrich) supplemented with 10% (v/v) fetal calf serum (Sigma-Aldrich) and penicillin-streptomycin (Gibco) and maintained in an incubator at 37°C under 5% CO_2. Cell lines were regularly tested for mycoplasma contamination. For siRNA transfection, Dharmafect-3 (Dharmacon) was used for U2OS cells, whereas Hiperfect (Qiagen) or Lipofectamine 2000 (Life Technologies) was used for HeLa cells. All siRNAs were made by Dharmacon (Lafayette, USA) or MWG (Munich, Germany). For DNA transfection, Fugene 6 (Promega) was used following manufacturer's guidelines.

Immunoprecipitations with GFP trap

For GFP-trap immunoprecipitations from HEK293 cells, 20 µg of plasmid DNA containing GFP-tagged bait were transfected into 15-cm dishes using polyethylenimine (PEI, Polysciences) in a 1:3 ratio. At 48 h post transfection, cells were lysed in 20 mM Tris-HCl, pH 7.8, 50 mM NaCl, 5 mM $MgCl_2$, 0.5% NP40, Roche EDTA-free protease inhibitor cocktail. After removing the cell debris, the lysates were incubated for 1 h with GFP-trap beads (Chromotek, Munich, Germany), followed by two washes in lysis buffer.

Immunofluorescence

For immunofluorescence, cells were fixed with 4% PFA solution in PBS, permeabilized with 0.1% saponin and blocked with 1% BSA in PBS before applying the indicated primary antibodies and corresponding fluorescently labelled secondary antibodies. All images, besides the images for the quantitative transferrin–Alexa-Fluor-488 recycling assay were acquired with a Leica TCS 8ST-WS confocal microscope. Images were analyzed and exported with the Volocity software package (Perkin Elmer). The Pearson's correlation between the respective channels was quantified with the colocalization tool of the Volocity software after the setting of uniform thresholds across conditions using the auto-threshold function of Volocity. The colocalization coefficient corresponds to the Mander's coefficient M2 calculated by the Volocity software after applying uniform thresholds across conditions using the Volocity auto-threshold function.

Autophagic flux assay

U2OS cells were infected with a lentivirus encoding GFP–LC3b, transfected with control siRNA and siRNA against ANKRD50, seeded onto coverslips and incubated for 72 h after transfection. Cells were then starved in complete Earl's buffered salt solution (EBSS, Sigma-Aldrich) with and without bafilomycin A1 (Sigma-Aldrich) for the indicated time points, followed by fixing in 4% PFA in PBS and nuclear counterstaining with DAPI. Representative images were acquired by confocal microscopy on a Leica SP8 microscope.

Flow cytometry of integrins

The flow-cytometry-based analysis of integrins has been described previously (Steinberg et al., 2012).

EGFR degradation assay

To measure EGFR degradation rates, HeLa cells were transfected with control siRNA and siRNA against ANKRD50, seeded into 12-well plates, grown to confluence and starved of serum overnight. The cells were then treated with 100 ng/ml EGF (Peprotech) for the indicated time points and lysed in 2% Triton X-100 in TBS with Roche Complete protease inhibitor. EGFR levels were then quantified by western blotting and analysis with an Odyssey SA scanner.

Transferrin recycling assay

U2OS cells were transfected with scrambled and ANKRD50-specific siRNAs, seeded onto coverslips and grown to confluence over 72 h. Cells were then incubated for 30 min with 20 µg/ml of Alexa-Fluor-488-labelled transferrin (Life Technologies) in serum-free DMEM, washed in cold PBS and stored on ice. Internalized transferrin was then chased in pre-warmed DMEM containing 10% FBS and 100 µg/ml unlabelled transferrin (Sigma-Aldrich) for the indicated time points. After the chase, cells were fixed in ice-cold 4% PFA for 30 min, followed by DAPI counterstaining and mounting. The transferrin content was then quantified as the average fluorescence intensity from ten images per condition acquired on a Zeiss AxioImager wide-field microscope.

Biotinylation-based GLUT1 degradation assay

The biotinylation-based degradation assay has been described previously (Steinberg et al., 2013).

SILAC interactome analysis

GFP and GFP–ANKRD50 were expressed using lentiviral infection of HEK293 and RPE1 cells, which were then grown in light non-isotope-labelled R0K0 medium (for GFP) or in arginine-10- and lysine-8- (Silantes, Munich, Germany) labelled heavy-isotope medium. GFP-trap isolation and subsequent analysis has been described previously (Steinberg et al., 2013, 2012).

Quantification of the surface proteome

To determine changes in the U2OS cell surface proteome, the cells were labelled with R0K0 and R10K8 DMEM for 14 days. ANKRD50 was depleted in a 6-well format using the Dharmacon On-Target Plus Smartpool of oligonucleotides against ANKRD50. 72 h after siRNA transfection, the cells were surface biotinylated using cleavable Sulfo-NHS-SS-Biotin (Apex Biotechnology, TX). Cells were lysed in PBS with 2% Triton X-100, and biotinylated membrane proteins were isolated with streptavidin–Sepharose™ (GE Healthcare). The beads were extensively washed with PBS containing 1.2 M NaCl and 1% Triton-X100 to remove as much unspecific binding as possible. Proteins were then eluted by boiling the beads in sample buffer containing DTT. The samples were further processed following the same protocol described in the SILAC interactome analysis.

Direct recombinant interaction studies

For all direct recombinant studies except the ANKRD50-D4 retromer trimer interaction, proteins were expressed as GST-fusion proteins using pGEX-6p-3 (GE Healthcare) in *E. coli* BL21 (NEB). Expression was induced with 0.1 mM IPTG for 16 h in 18°C. Proteins were isolated from lysates made with PBS containing 1% Triton X-100 and lysed using sonication. The cell lysate was cleared using centrifugation and incubated with glutathione–Sepharose™ 4B beads (GE Healthcare) to pull down the proteins of interest. The bait was left on the beads as GST-fusion proteins, and the potential interacting protein was cleaved from the GST beads using PreScission Protease (GE Healthcare) according to the manufacturer's instructions. The binding reaction was then assayed in 20 mM Tris-HCl, pH 7.8, 100 mM NaCl, 0.5% NP40, 0.1% BSA. For the ANKRD50-D4 and retromer trimer interaction, D4 was expressed as a GST-fusion protein that remained bound to the glutathione beads as described above. The retromer trimer was produced with the pSecTag2 mammalian secretion system (Invitrogen). For that, VPS26, VPS29 and VPS35 were cloned with an N-terminal HA-tag into the pSectag2 plasmid, so that the pSecTag2 Igκ leader sequence ensures secretion of the proteins. Plasmids were either pooled as indicated in the figure or individually transfected into 15-cm dishes of HEK293 cells, followed by 72 h of incubation in full growth DMEM. The beads with GST, GST–ANKRD50-D4 and GST–ANKRD50-D4-E1300A were then directly incubated with the filtered tissue culture supernatant and washed three times in 20 mM Tris-HCl, pH 7.8, 100 mM NaCl, 0.5% NP40, 0.1% BSA followed by boiling in sample buffer. One third of the beads was loaded onto a gel for the Coomassie-stained GST input images, two thirds were loaded onto a separate gel to detect HA-tagged VPS proteins.

siRNA

ANKRD50 expression was suppressed with four siRNAs found in the OnTarget Plus Smartpool from Dharmacon. VPS35, SNX27, WASH1 and FAM21 were suppressed with reagents that have been published previously (Steinberg et al., 2013; Zech et al., 2011).

Rescue of SLC1A4 lysosomal mis-sorting with ANKRD50 constructs

HeLa cells transduced with lentiviruses to express mCherry–SLC1A4 and the GFP-tagged ANKRD50 rescue constructs were transfected with the siRNA ANKRD50-2 to suppress endogenous ANKRD50 expression. Cells were fixed and stained 72 h after siRNA transfection. LAMP1 and SLC1A4 colocalization was analyzed by confocal microscopy on a Leica SP8 microscope followed by image analysis with Volocity software.

Acknowledgements

Special thanks go to Roland Nitschke and Angela Naumann of the Life Imaging Center (LIF) of Freiburg University for their help in all imaging-related protocols.

Competing interests

The authors declare no competing or financial interests.

Author contributions

A.K. and F.S. performed most of the lab work. A.J.O. performed some of the molecular biology work and selected image acquisition. H.N. helped with some of the molecular biology work and tissue culture. K.J.H., B.D. and J.D. analyzed the proteomics samples by mass spectrometry. F.S. and P.J.C. designed the study, supervised the work and wrote the manuscript.

Funding

The work was funded by the German Research Council (Deutsche Forschungsgemeinschaft) Emmy Noether grant (STE2310/1-1 to F.S.); Wellcome Trust grants to P.J.C. (089928, 086777 and 093549). J.D. is funded by the Swiss National Science Foundation (Schweizerischer Nationalfonds zur Förderung der Wissenschaftlichen Forschung) (31003A-166482/1). Deposited in PMC for release after 6 months.

Supplementary information

Supplementary information available online at
http://jcs.biologists.org/lookup/doi/10.1242/jcs.196758.supplemental

References

Bottcher, R. T., Stremmel, C., Meves, A., Meyer, H., Widmaier, M., Tseng, H. Y. and Fassler, R. (2012). Sorting nexin 17 prevents lysosomal degradation of beta (1) integrins by binding to the beta(1)-integrin tail. *Nat. Cell Biol.* **14**, 584-592.

Burd, C. and Cullen, P. J. (2014). Retromer: a master conductor of endosome sorting. *Cold Spring Harb. Perspect. Biol.* **6**.

Cai, L., Loo, L. S., Atlashkin, V., Hanson, B. J. and Hong, W. (2011). Deficiency of sorting nexin 27 (SNX27) leads to growth retardation and elevated levels of N-methyl-D-aspartate receptor 2C (NR2C). *Mol. Cell. Biol.* **31**, 1734-1747.

Chan, A. S. M., Clairfeuille, T., Landao-Bassonga, E., Kinna, G., Ng, P. Y., Loo, L. S., Cheng, T. S., Zheng, M., Hong, W., Teasdale, R. D. et al. (2016). Sorting nexin 27 couples PTHR trafficking to retromer for signal regulation in osteoblasts during bone growth. *Mol. Biol. Cell* **27**, 1367-1382.

Derivery, E., Sousa, C., Gautier, J. J., Lombard, B., Loew, D. and Gautreau, A. (2009). The Arp2/3 activator WASH controls the fission of endosomes through a large multiprotein complex. *Dev. Cell* **17**, 712-723.

Duleh, S. N. and Welch, M. D. (2012). Regulation of integrin trafficking, cell adhesion, and cell migration by WASH and the Arp2/3 complex. *Cytoskeleton* **69**, 1047-1058.

Fjorback, A. W., Seaman, M., Gustafsen, C., Mehmedbasic, A., Gokool, S., Wu, C., Militz, D., Schmidt, V., Madsen, P., Nyengaard, J. R. et al. (2012). Retromer binds the FANSHY sorting motif in SorLA to regulate amyloid precursor protein sorting and processing. *J. Neurosci.* **32**, 1467-1480.

Gallon, M., Clairfeuille, T., Steinberg, F., Mas, C., Ghai, R., Sessions, R. B., Teasdale, R. D., Collins, B. M. and Cullen, P. J. (2014). A unique PDZ domain and arrestin-like fold interaction reveals mechanistic details of endocytic recycling by SNX27-retromer. *Proc. Natl. Acad. Sci. USA* **111**, E3604-E3613.

Ghai, R., Bugarcic, A., Liu, H., Norwood, S. J., Skeldal, S., Coulson, E. J., Li, S. S.-C., Teasdale, R. D. and Collins, B. M. (2013). Structural basis for endosomal trafficking of diverse transmembrane cargos by PX-FERM proteins. *Proc. Natl. Acad. Sci. USA* **110**, E643-E652.

Gomez, T. S. and Billadeau, D. D. (2009). A FAM21-containing WASH complex regulates retromer-dependent sorting. *Dev. Cell* **17**, 699-711.

Gomez, T. S., Gorman, J. A., De Narvajas, A. A.-M., Koenig, A. O. and Billadeau, D. D. (2012). Trafficking defects in WASH-knockout fibroblasts originate from collapsed endosomal and lysosomal networks. *Mol. Biol. Cell* **23**, 3215-3228.

Harbour, M. E., Breusegem, S. Y. A., Antrobus, R., Freeman, C., Reid, E. and Seaman, M. N. J. (2010). The cargo-selective retromer complex is a recruiting hub for protein complexes that regulate endosomal tubule dynamics. *J. Cell Sci.* **123**, 3703-3717.

Harbour, M. E., Breusegem, S. Y. and Seaman, M. N. J. (2012). Recruitment of the endosomal WASH complex is mediated by the extended 'tail' of Fam21 binding to the retromer protein Vps35. *Biochem. J.* **442**, 209-220.

Harrison, M. S., Hung, C.-S., Liu, T.-T., Christiano, R., Walther, T. C. and Burd, C. G. (2014). A mechanism for retromer endosomal coat complex assembly with cargo. *Proc. Natl. Acad. Sci. USA* **111**, 267-272.

Hussain, N. K., Diering, G. H., Sole, J., Anggono, V. and Huganir, R. L. (2014). Sorting Nexin 27 regulates basal and activity-dependent trafficking of AMPARs. *Proc. Natl. Acad. Sci. USA* **111**, 11840-11845.

Jia, D., Gomez, T. S., Metlagel, Z., Umetani, J., Otwinowski, Z., Rosen, M. K. and Billadeau, D. D. (2010). WASH and WAVE actin regulators of the Wiskott-Aldrich syndrome protein (WASP) family are controlled by analogous structurally related complexes. *Proc. Natl. Acad. Sci. USA* **107**, 10442-10447.

Jia, D., Gomez, T. S., Billadeau, D. D. and Rosen, M. K. (2012). Multiple repeat elements within the FAM21 tail link the WASH actin regulatory complex to the retromer. *Mol. Biol. Cell* **23**, 2352-2361.

Kallberg, M., Wang, H., Wang, S., Peng, J., Wang, Z., Lu, H. and Xu, J. (2012). Template-based protein structure modeling using the RaptorX web server. *Nat. Protoc.* **7**, 1511-1522.

Lauffer, B. E. L., Melero, C., Temkin, P., Lei, C., Hong, W., Kortemme, T. and von Zastrow, M. (2010). SNX27 mediates PDZ-directed sorting from endosomes to the plasma membrane. *J. Cell Biol.* **190**, 565-574.

Lee, S., Chang, J. and Blackstone, C. (2016). FAM21 directs SNX27-retromer cargoes to the plasma membrane by preventing transport to the Golgi apparatus. *Nat. Commun.* **7**, 10939.

Loo, L. S., Tang, N., Al-Haddawi, M., Dawe, G. S. and Hong, W. (2014). A role for sorting nexin 27 in AMPA receptor trafficking. *Nat. Commun.* **5**, 3176.

McGarvey, J. C., Xiao, K., Bowman, S. L., Mamonova, T., Zhang, Q., Bisello, A., Sneddon, W. B., Ardura, J. A., Jean-Alphonse, F., Vilardaga, J.-P. et al. (2016). Actin-Sorting Nexin 27 (SNX27)-retromer complex mediates rapid parathyroid hormone receptor recycling. *J. Biol. Chem.* **291**, 10986-11002.

McGough, I. J., Steinberg, F., Gallon, M., Yatsu, A., Ohbayashi, N., Heesom, K. J., Fukuda, M. and Cullen, P. J. (2014a). Identification of molecular heterogeneity in SNX27-retromer-mediated endosome-to-plasma-membrane recycling. *J. Cell Sci.* **127**, 4940-4953.

McGough, I. J., Steinberg, F., Jia, D., Barbuti, P. A., McMillan, K. J., Heesom, K. J., Whone, A. L., Caldwell, M. A., Billadeau, D. D., Rosen, M. K. et al. (2014b). Retromer binding to FAM21 and the WASH complex is perturbed by the parkinson disease-linked VPS35(D620N) mutation. *Curr. Biol.* **24**, 1670-1676.

McGough, I. J., Steinberg, F., Jia, D., Barbuti, P. A., McMillan, K. J., Heesom, K. J., Whone, A. L., Caldwell, M. A., Billadeau, D. D., Rosen, M. K. et al. (2014c). Retromer binding to FAM21 and the WASH complex is perturbed by the parkinson disease-linked VPS35(D620N) mutation (vol 24, pg 1670, 2014). *Curr. Biol.* **24**, 1678-1678.

Phillips-Krawczak, C. A., Singla, A., Starokadomskyy, P., Deng, Z., Osborne, D. G., Li, H., Dick, C. J., Gomez, T. S., Koenecke, M., Zhang, J.-S. et al. (2015). COMMD1 is linked to the WASH complex and regulates endosomal trafficking of the copper transporter ATP7A. *Mol. Biol. Cell* **26**, 91-103.

Piotrowski, J. T., Gomez, T. S., Schoon, R. A., Mangalam, A. K. and Billadeau, D. D. (2013). WASH knockout T cells demonstrate defective receptor trafficking, proliferation, and effector function. *Mol. Cell. Biol.* **33**, 958-973.

Seaman, M. N. J. (2007). Identification of a novel conserved sorting motif required for retromer-mediated endosome-to-TGN retrieval. *J. Cell Sci.* **120**, 2378-2389.

Seaman, M. N. J. (2012). The retromer complex - endosomal protein recycling and beyond. *J. Cell Sci.* **125**, 4693-4702.

Seaman, M. N. J., Mccaffery, J. M. and Emr, S. D. (1998). A membrane coat complex essential for endosome-to-Golgi retrograde transport in yeast. *J. Cell Biol.* **142**, 665-681.

Seaman, M. N. J., Harbour, M. E., Tattersall, D., Read, E. and Bright, N. (2009). Membrane recruitment of the cargo-selective retromer subcomplex is catalysed by the small GTPase Rab7 and inhibited by the Rab-GAP TBC1D5. *J. Cell Sci.* **122**, 2371-2382.

Steinberg, F., Heesom, K. J., Bass, M. D. and Cullen, P. J. (2012). SNX17 protects integrins from degradation by sorting between lysosomal and recycling pathways. *J. Cell Biol.* **197**, 219-230.

Steinberg, F., Gallon, M., Winfield, M., Thomas, E. C., Bell, A. J., Heesom, K. J., Tavaré, J. M. and Cullen, P. J. (2013). A global analysis of SNX27-retromer assembly and cargo specificity reveals a function in glucose and metal ion transport. *Nat. Cell Biol.* **15**, 461-471.

Tabuchi, M., Yanatori, I., Kawai, Y. and Kishi, F. (2010). Retromer-mediated direct sorting is required for proper endosomal recycling of the mammalian iron transporter DMT1. *J. Cell Sci.* **123**, 756-766.

Temkin, P., Lauffer, B., Jäger, S., Cimermancic, P., Krogan, N. J. and von Zastrow, M. (2011). SNX27 mediates retromer tubule entry and endosome-to-plasma membrane trafficking of signalling receptors. *Nat. Cell Biol.* **13**, 717-723.

Vilarino-Guell, C., Wider, C., Ross, O. A., Dachsel, J. C., Kachergus, J. M., Lincoln, S. J., Soto-Ortolaza, A. I., Cobb, S. A., Wilhoite, G. J., Bacon, J. A. et al. (2011). VPS35 mutations in Parkinson disease. *Am. J. Hum. Genet.* **89**, 162-167.

Wang, X., Zhao, Y., Zhang, X., Badie, H., Zhou, Y., Mu, Y., Loo, L. S., Cai, L., Thompson, R. C., Yang, B. et al. (2013). Loss of sorting nexin 27 contributes to excitatory synaptic dysfunction by modulating glutamate receptor recycling in Down's syndrome. *Nat. Med.* **19**, 473-480.

Wen, L., Tang, F.-L., Hong, Y., Luo, S.-W., Wang, C.-L., He, W., Shen, C., Jung, J.-U., Xiong, F., Lee, D.-H. et al. (2011). VPS35 haploinsufficiency increases Alzheimer's disease neuropathology. *J. Cell Biol.* **195**, 765-779.

Zavodszky, E., Seaman, M. N. J., Moreau, K., Jimenez-Sanchez, M., Breusegem, S. Y., Harbour, M. E. and Rubinsztein, D. C. (2014). Mutation in VPS35 associated with Parkinson's disease impairs WASH complex association and inhibits autophagy. *Nat. Commun.* **5**, 3828.

Zech, T., Calaminus, S. D. J., Caswell, P., Spence, H. J., Carnell, M., Insall, R. H., Norman, J. and Machesky, L. M. (2011). The Arp2/3 activator WASH regulates alpha5beta1-integrin-mediated invasive migration. *J. Cell Sci.* **124**, 3753-3759.

Zimprich, A., Benet-Pagès, A., Struhal, W., Graf, E., Eck, S. H., Offman, M. N., Haubenberger, D., Spielberger, S., Schulte, E. C., Lichtner, P. et al. (2011). A mutation in VPS35, encoding a subunit of the retromer complex, causes late-onset Parkinson disease. *Am. J. Hum. Genet.* **89**, 168-175.

Supplementary Figures:

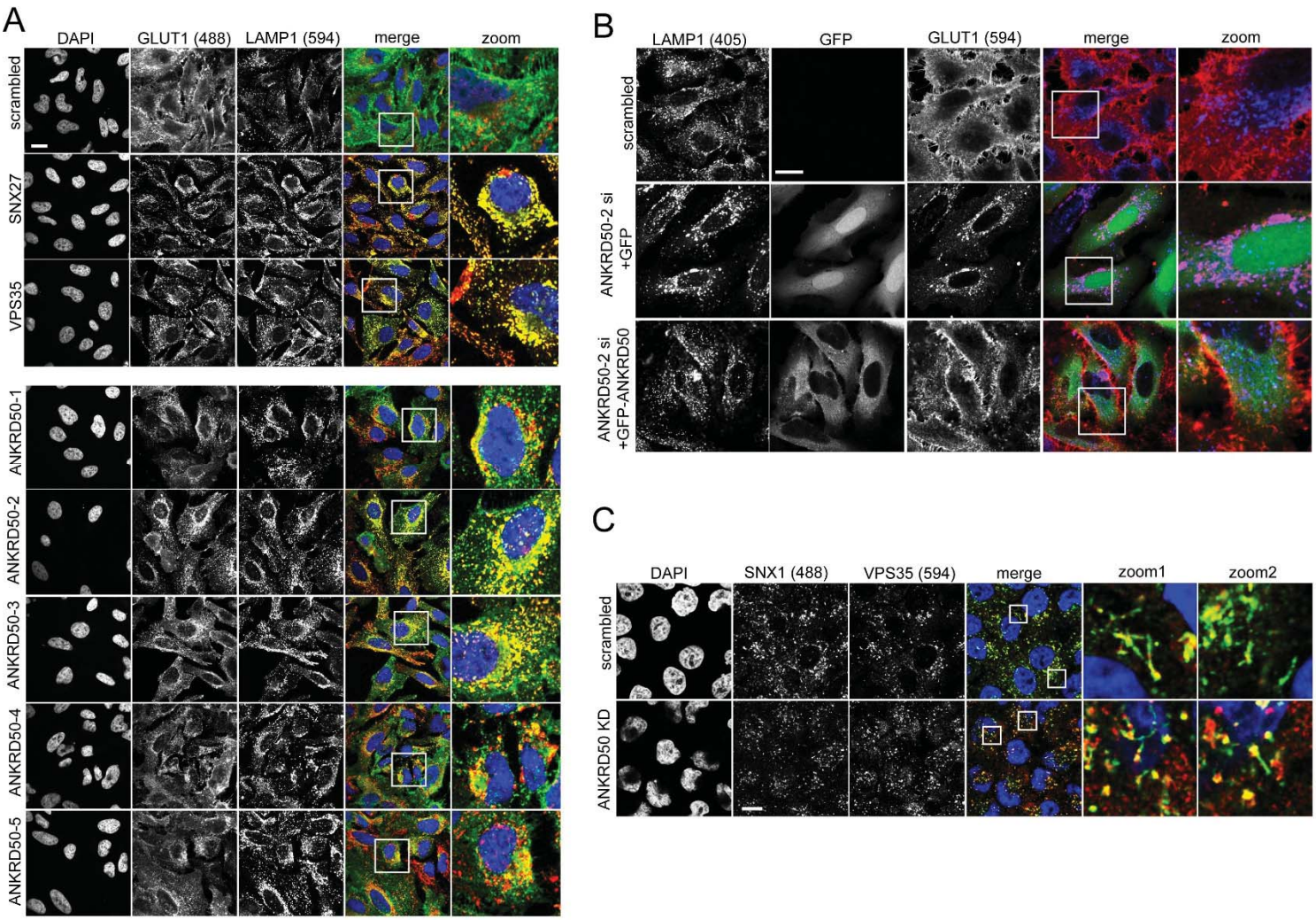

Figure S1: A: HeLa cells were transfected with the indicated siRNAs, fixed 72h post transfection and stained for endogenous GLUT1 and LAMP1. **B:** Hela cells expressing GFP and siRNA resistant GFP-ANKRD50 were transfected with siRNA ANKRD50-2 and stained for endogenous GLUT1 and LAMP1 to test whether GFP-ANKRD50 rescued GLUT1 lysosomal mis-sorting. **C:** U2OS cells were transfected with siRNA against ANKRD50 and stained for endogenous SNX1 and VPS35. The two magnified areas highlight areas of observed SNX1 positive tubulation. All scale bars = 10µm.

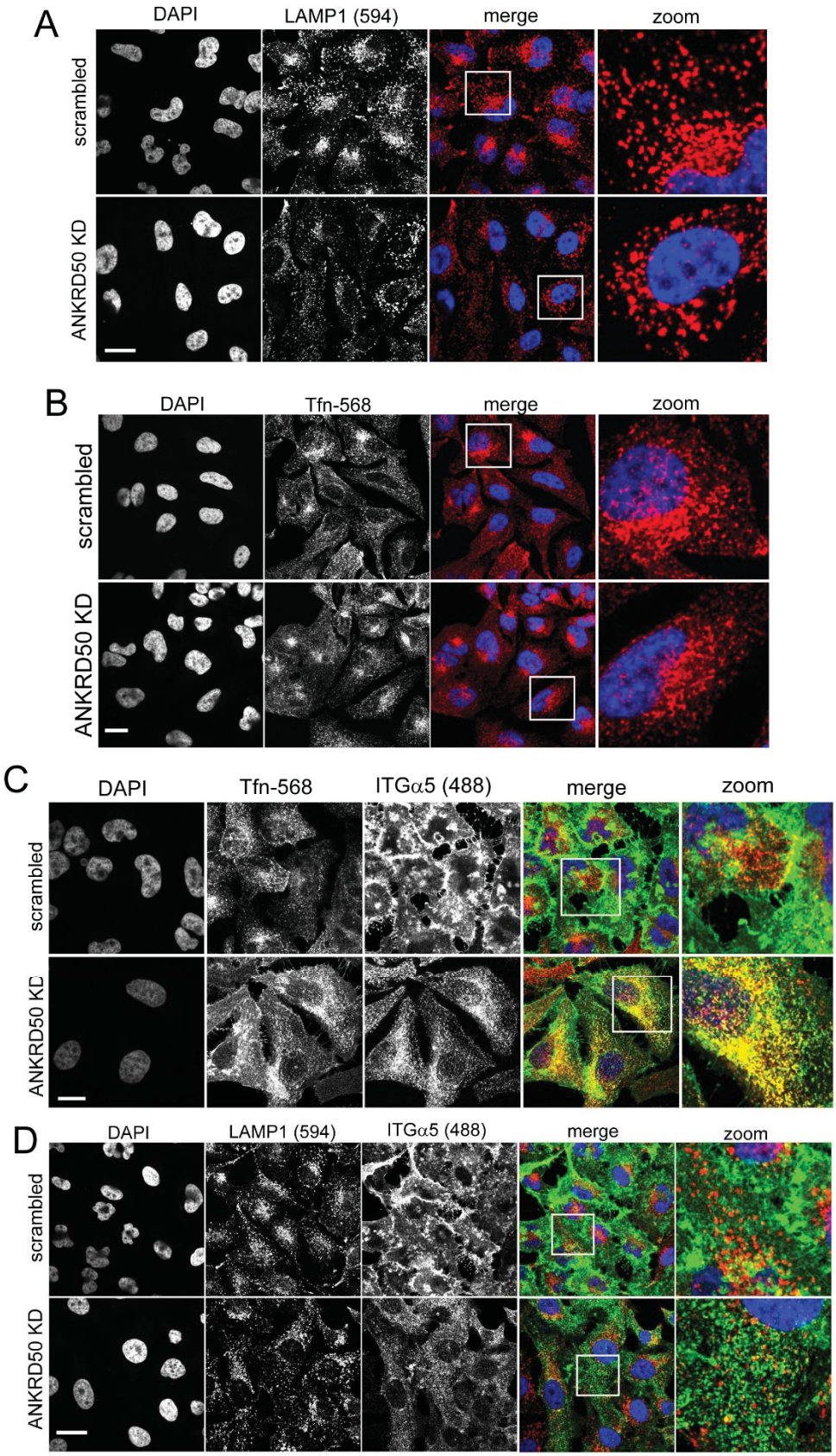

Figure S2: A: HeLa cells were transfected with ANKRD50 siRNA, fixed 72h post transfection and stained for the lysosomal marker protein LAMP1. **B**: HeLa cells were transfected with ANKRD50 siRNA and incubated with Alexa-568 labeled transferrin for 30min to visualize the endocytic recycling compartment, followed by fixation and nuclear staining with DAPI. All scale bars = 10µm.

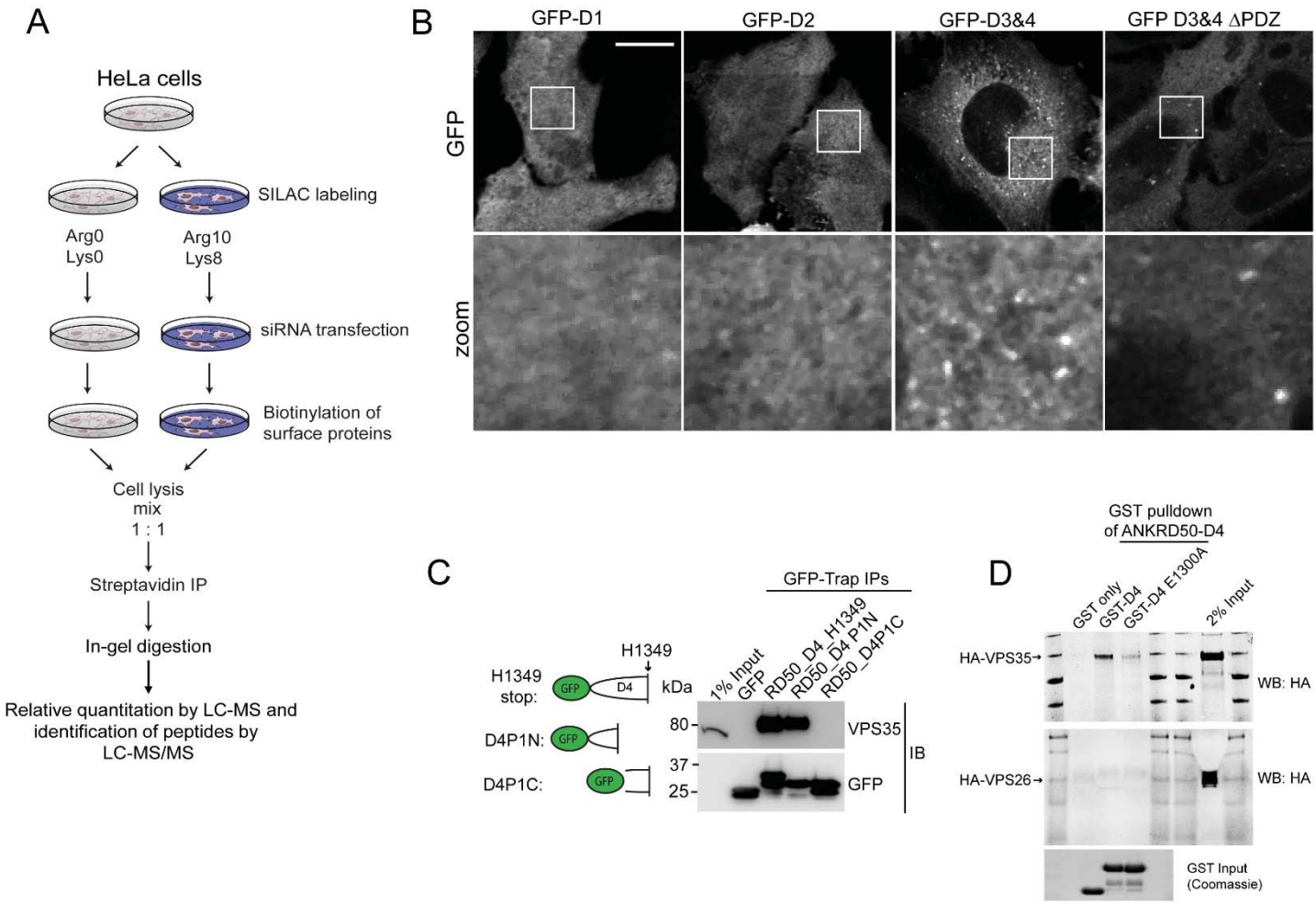

Figure S3: A: Schematic representation of the SILAC workflow to quantify the surface proteome of ANKRD50 depleted U2OS cells. **B**: High magnification panel of the GFP channel shown in Figure 6F. Note that GFP-D3&4 displays vesicular localization, which is largely but not completely lost when the PDZ ligand is truncated (GFP-D3&4 ΔPDZ). Scale bar = 10µm. **C:** The D4-P1N fragment with amino acids from 1292-1320 efficiently precipitate VPS35 while the fragment D4-P1C from AAs 1320-1349 loses binding. **D:** GST-tagged ANKRD50-D4 but not the retromer binding mutant GST-D4-E1300A produced in bacteria binds to the pSecTag2 (secreted as soluble proteins into the tissue culture supernatant of HEK293 cells) expressed HA-tagged retromer subunit VPS35 but not to the retromer subunit VPS26.

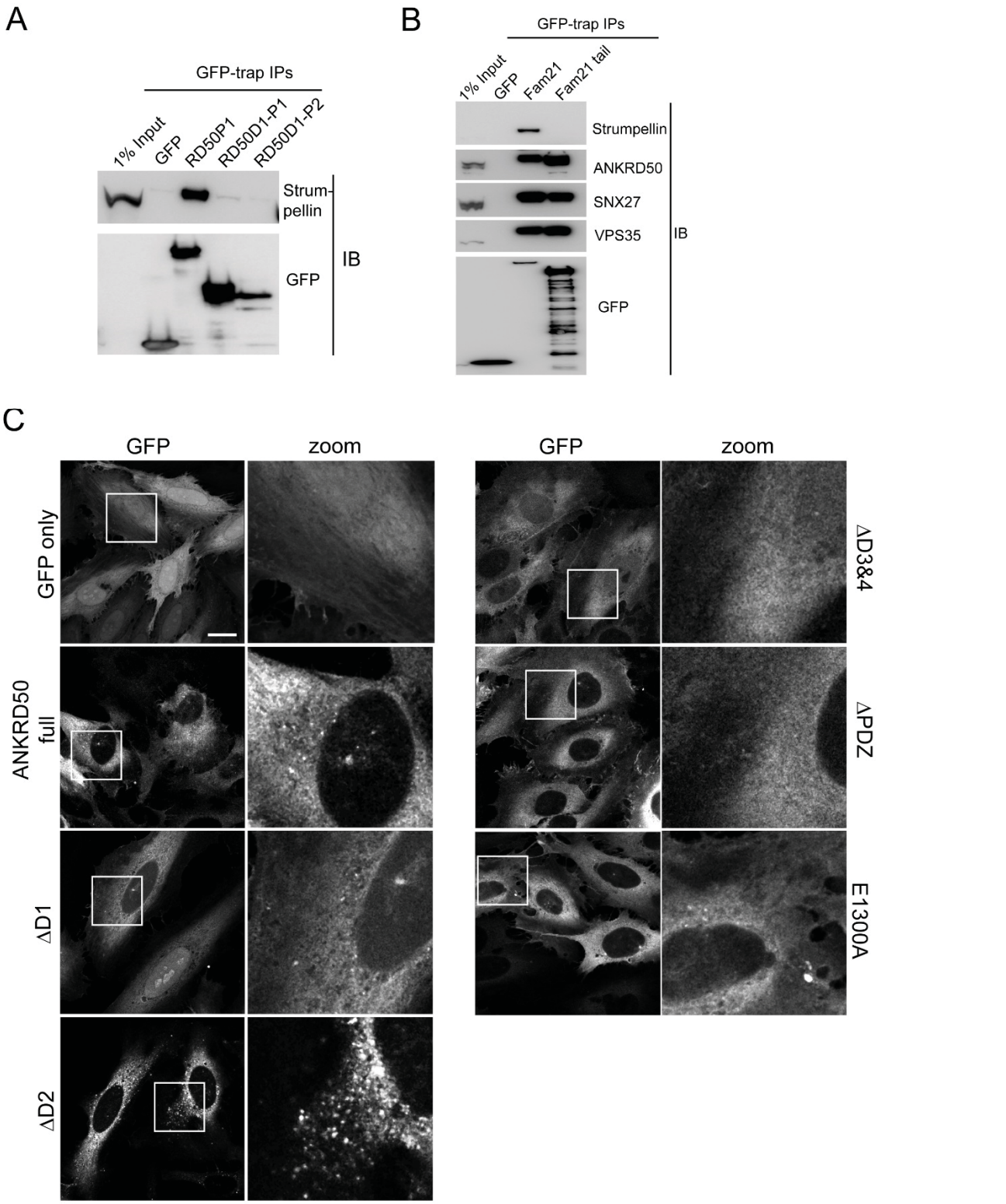

Figure S4: A: HEK293 cells were transiently transfected with GFP-tagged ANKRD50-D1 and ANKRD50-D1 split into two equal parts (D1-P1= AAs 1-238, D1-P2= AAs 239-476), followed by GFP-trap IP and detection of WASH complex component Strumpellin in the precipitates. **B:** GFP-tagged Fam21 full length and the Fam21 tail region were precipitated from HEK293 cells and analyzed for binding to the indicated proteins by western blotting of the precipitates. **C:** Hela cells transduced with the indicated siRNA resistant ANKRD50 constructs were transfected with ANKRD50-2 siRNA and vesicular localization of the GFP-ANKRD50 variants examined. Scale bar = 10µm.